Geological Quarterly, 2022, 66: 8
DOI: http://dx.doi.org/10.7306/gq.1640

Revision of the trace fossil *Megagrapton* Książkiewicz, 1968 with focus on *Megagrapton aequale* Seilacher, 1977 from the lower Eocene of the Lesser Caucasus in Georgia

Alfred UCHMAN[1, *], Zurab LEBANIDZE[2], Tamar BERIDZE[3], Nino KOBAKHIDZE[3], Koba LOBZHANIDZE[3], Davit MAKADZE[5], Sophio KHUTSISHVILI[3], Rusudan CHAGELISHVILI[4], Kakha KOIAVA[2] and Nino KHUNDADZE[5]

[1] Jagiellonian University, Institute of Geological Sciences, Gronostajowa 3a, 30-387 Kraków, Poland

[2] Iv. Javakhishvili Tbilisi State University, Faculty of Exact and Natural Sciences, University 13, 0186 Tbilisi, Georgia

[3] Iv. Javakhishvili Tbilisi State University, Alexander Janelidze Institute of Geology, Politkovskaia 31, 0186 Tbilisi, Georgia

[4] Department of Geology and Paleontology, Georgian National Museum, 3, Purtseladze, 0105 Tbilisi, Georgia

[5] Tbilisi State University, Alexander Tvalchrelidze Caucasian Institute of Mineral Resources, 12, Mindeli, 0186 Tbilisi, Georgia

Uchman, A., Lebanidze, Z., Beridze, T., Kobakhidze, N., Lobzhanidze, K., Makadze, D., Khutsishvili, S., Chagelishvili, R., Koiava, K., Khundadze, N., 2022. Revision of the trace fossil *Megagrapton* Książkiewicz, 1968 with focus on *Megagrapton aequale* Seilacher, 1977 from the lower Eocene of the Lesser Caucasus in Georgia. Geological Quarterly, 2022, 66: 8, doi: 10.7306/gq.1640

Megagrapton Książkiewicz, 1968 is a characteristic deep-sea trace fossil belonging to the group of graphoglyptids and mostly preserved as a network of irregular meshes in hypichnial semirelief. So far, eleven ichnospecies have been distinguished under this ichnogenus, though commonly on weak evidence. The so-far poorly known ichnospecies *Megagrapton aequale* Seilacher, 1977 is described here on the basis of the numerous, newly discovered specimens from deep-sea siliciclastic deposits of the Bolevani Subsuite (lower Eocene) in the Lesser Caucasus of Georgia, together with other collections and published examples. A neotype of this ichnospecies is designated and the diagnosis emended. *M. aequale* occurs in lower Cambrian to upper Miocene deep-sea turbiditic deposits, mostly in the Paleogene. It is characterized by relatively small, variable meshes, which have mostly irregular sub-pentagonal, sub-hexagonal or sub-heptagonal shapes that are variable in size and are bordered by curved or straight semicircular ridges. It has been mistaken for *Paleodictyon,* which forms regular hexagonal nets. *Paleodictyon imperfectum* Seilacher, 1977 is included in *M. aequale* as the ichnosubspecies *M. a. imperfectum*, which is characterized by relatively thin bordering ridges. After critical analysis of all ichnospecies, only *M. irregulare* Książkiewicz, 1968, *M. submontanum* (Azpeitia Moros, 1933), and *M. aequale* are recommended for further use. These are distinguished on the basis of the prevailing morphology of the meshes, irrespective of large differences in morphometric parameters within the ichnospecies. *Irredictyon chaos* Vialov, 1972 is included in *M. irregulare* as the ichnosubspecies *M. i. chaos*, which is characterized by relatively thick bordering ridges. *Megagrapton* is interpreted as a cast of a subsurface open burrow network with a few connections to the sea floor. The burrows probably functioned as a trap for small organisms (ethological subcategory irretichnia).

Key words: ichnology, flysch, ichnotaxonomy, graphoglyptids, Paleogene.

INTRODUCTION

The trace fossil *Megagrapton* Książkiewicz, 1968 is a characteristic component of the deep-sea patterned trace fossils called graphoglyptids (Seilacher, 1977). It is composed of semicircular ridges forming a net with irregular meshes that is usually preserved in semirelief on the sole of turbiditic sandstones (Książkiewicz, 1977). Differences in mesh shape, real or alleged, has led to the erection of eleven ichnospecies, including *Megagrapton irregulare* Książkiewicz, 1968, *M. submontanum* (Azpeitia Moros, 1933), *M. aequale* Seilacher, 1977, *M. regulare* Ghare and Badve, 1977, *M. tibeticum* Yang and Song, 1985, *M. angulare* Stepanek and Geyer, 1989, *M. permicum* Kozur et al., 1996, *M. transitum* Kozur et al., 1997, *M. fornicatum* Kappel, 2003, and *M. fupingensis* Yang et al., 2004. However, other ichnogenera, such as *Pseudopaleodictyon* Pfeiffer, 1968, typified by *P. hartungi* (Geinitz, 1867), and *Multina* Orłowski, 1968, typified by *Multina magna* Orłowski, 1968, also show irregular polygons but common overcrossings (Uchman, 1998) and preservation in full relief. Their distinction may cause problems. Better understanding requires further studies, but several problems appear within the ichnogenus *Megagrapton,* which should be resolved prior to making further steps. Foremost among them, the

* Corresponding author, e-mail: alfred.uchman@uj.edu.pl
Received: February 7, 2022; accepted: March 2, 2022; first published online: June 24, 2022

internal variability of the *Megagrapton* ichnospecies is poorly known, especially with respect to these that are only represented by only a few specimens.

Among the *Megagrapton* ichnospecies, *M. aequale* has been known only from a drawing based on a field photograph of a single uncollected specimen (Seilacher, 1977: fig. 11e) and without closely constrained facies context. The specimen in the drawing was originally designated as the holotype, such situation being unacceptable in current ichnotaxonomy and in taxonomy generally. In this paper, *M. aequale* from the lower Eocene deep-sea deposits of the Lesser Caucasus in Georgia is described from abundant occurrences in some beds in two well-documented sections (Ardagani-3 and Ormotsi-1). The new material from the Lesser Caucasus and some other material from different collections, including material from the type area, mostly from deep-sea Cretaceous-Paleogene deposits, allow better characterization of this ichnospecies as regards its morphology and palaeoenvironment. The literature survey and inspection of several European collections now allows recognition of *M. aequale* in other areas and deposits of different ages.

The study also gives an opportunity for a reassessment of the other *Megagrapton* ichnospecies, which is undertaken in this paper on the basis of the literature and inspection of several collections. On this basis, new or modified criteria for distinction of *Megagrapton* ichnospecies are provided. The taxonomic revision of *Megagrapton* is important for deep-sea ichnology because of several inconsistencies in the literature, which otherwise would be multiplied. Furthermore, the ethological and palaeoenvironmental interpretations of *Megagrapton* are summarized.

GEOLOGICAL SETTING

GENERAL BACKGROUND

The study area is located in the Lesser Caucasus. It belongs to the northern Tethyan geological province (Zakariadze et al., 2007, 2012). The study sections are located in the Achara-Trialeti Fold-and-Thrust Belt (ATFTB), south of the northern Transcaucasian (Georgian and Azerbaijanian) blocks and north of the Lower Paleogene Middle East andesitic belt. The ATFTB is partly overlain by Oligocene-Neogene deposits of the River Mtkvari (Kura) intermontane depression and by young volcanic rocks (Adamia et al., 2015; Fig. 1A). The ATFTB resulted from the structural inversion of a back-arc rift basin, the likely eastward prolongation of the eastern Black Sea, which opened in Cretaceous-Eocene times (Adamia et al., 1974, 2002; Banks et al., 1997; Sosson et al., 2016; Alania et al., 2021). Late Alpine inversion of the Achara-Trialeti extensional basin is associated with the Arabia-Eurasia convergence (Banks et al., 1997; Sosson et al., 2016; Alania et al., 2017).

Deposits constituting the ATFTB accumulated in the Achara-Trialeti extensional trough-like basin during Late Cretaceous-Eocene times. Aptian and Albian volcanogenic-sedimentary formations are the oldest units of the trough (Gamkrelidze, 1964; Lordkipanidze et al., 1989; Nadareishvili, 1999). These are overlain by Cenomanian-Maastrichtian alternations of volcanogenic and carbonate rocks and Paleocene (Danian) marls. The upper Paleocene (Thanetian) and lower Eocene (Ypresian) stages are mainly represented by clastic turbidites, which are ascribed to the Borjomi Flysch or Borjomi Suite (Fig. 2; Obruchev, 1923; Gamkrelidze, 1949).

The Borjomi area is typical of the Paleocene-lower Eocene Borjomi Flysch also called the Borjomi Suite. The Borjomi Suite is subdivided into the Tusrebi, Boshuri and Bolevani subsuites (Beradze et al., 1985). The Paleocene (Thanetian) Tusrebi Subsuite constitutes nearly three-quarters (900–1000 m) of the entire thickness of the Borjomi Flysch. According to recent field observations (Uchman et al., 2020), it can be subdivided into three lithofacies units:

- lower Tusrebi shaly unit formed by packages composed of mudstones (often marly), siltstones and very fine-grained sandstones;
- middle Tusrebi sandy unit consisting of sandy packages separated by shaly intercalations;
- upper Tusrebi shaly unit.

The volcanogenic-sedimentary Boshuri Subsuite contains deformed (slumped) deposits rich in volcanic material and related debris-flow deposits, graded sandstones (typical turbidites) and amalgamated massive sandstones interbedded with mudstones and siltstones. In some cases, thick intervals of amalgamated sandstones include thin intercalations of locally laminated mudstone or siltstone. Some silty laminae mark amalgamation surfaces.

The mostly shaly Bolevani Subsuite is formed by deep-sea heterolithic deposits (thin alternations of mudstones, siltstones and sandstones with pelagites/hemipelagites). It is dated to the lower Eocene (Ypresian). The Bolevani Subsuite, 150–180 m thick, terminates the Borjomi Suite. Its key section was described 4 km NW from the Ardagani-3 section in the same southern flank of the Borjomi Anticline, where it is subdivided into lower and upper marly (shaly) units with a sandy (mainly sandstones) unit in between (Beradze et al., 1985). In other parts of the Borjomi region, the Bolevani Subsuite is not subdivided as the middle sandy part is not well exposed.

The Borjomi Suite is conformably overlain by ~2000–3000 m thick middle Eocene volcanic and volcanogenic deposits. According to previous studies, the lower Eocene part of the Borjomi Flysch was deposited under shallow marine and hemipelagic conditions (Yilmaz et al., 2001). However, newer interpretations point to a deep-sea palaeoenvironment (Lebanidze et al., 2019; Uchman et al., 2020; Beridze et al., 2021).

SECTIONS STUDIED

The Ardagani-3 section studied represents a part of the Paleocene-lower Eocene Borjomi Suite on the southern flank of the Borjomi Anticline, which is one of the important fold structures of the central ATFTB (Fig. 1B). It is located by the Ardagani settlement along the Borjomi-Bakuriani road (GPS coordinates: 41°49.187’N, 043°24.414’E; 857 m a.s.l.; see Fig. 1B), SE of the Ardagani-1 section (see Uchman et al., 2020) and represents the lower Eocene volcanogenic-sedimentary Boshuri and the shaly Bolevani subsuites. The Ardagani 3 section (Fig. 3) is ~98 m thick. It incorporates the uppermost part of the Boshuri Subsuite (approximately the first 41 m of the section) and the lower-middle parts of the Bolevani Subsuite (~57 m thick). The lower part of the section comprises sandstone beds (from several cm to 50 cm thick) alternating with siltstones and mudstones. The sandstones are tuffaceous, containing abundant volcanic material. They are very fine- to fine-grained, commonly parallel, rarely wavy laminated, and ripple-cross and/or cross laminated at the tops of beds, with local convolute, dish and water escape structures. Some beds show transitions from fine grained sandstone to siltstone. Flute casts on the lower surface of some sandstone beds point to transpor-

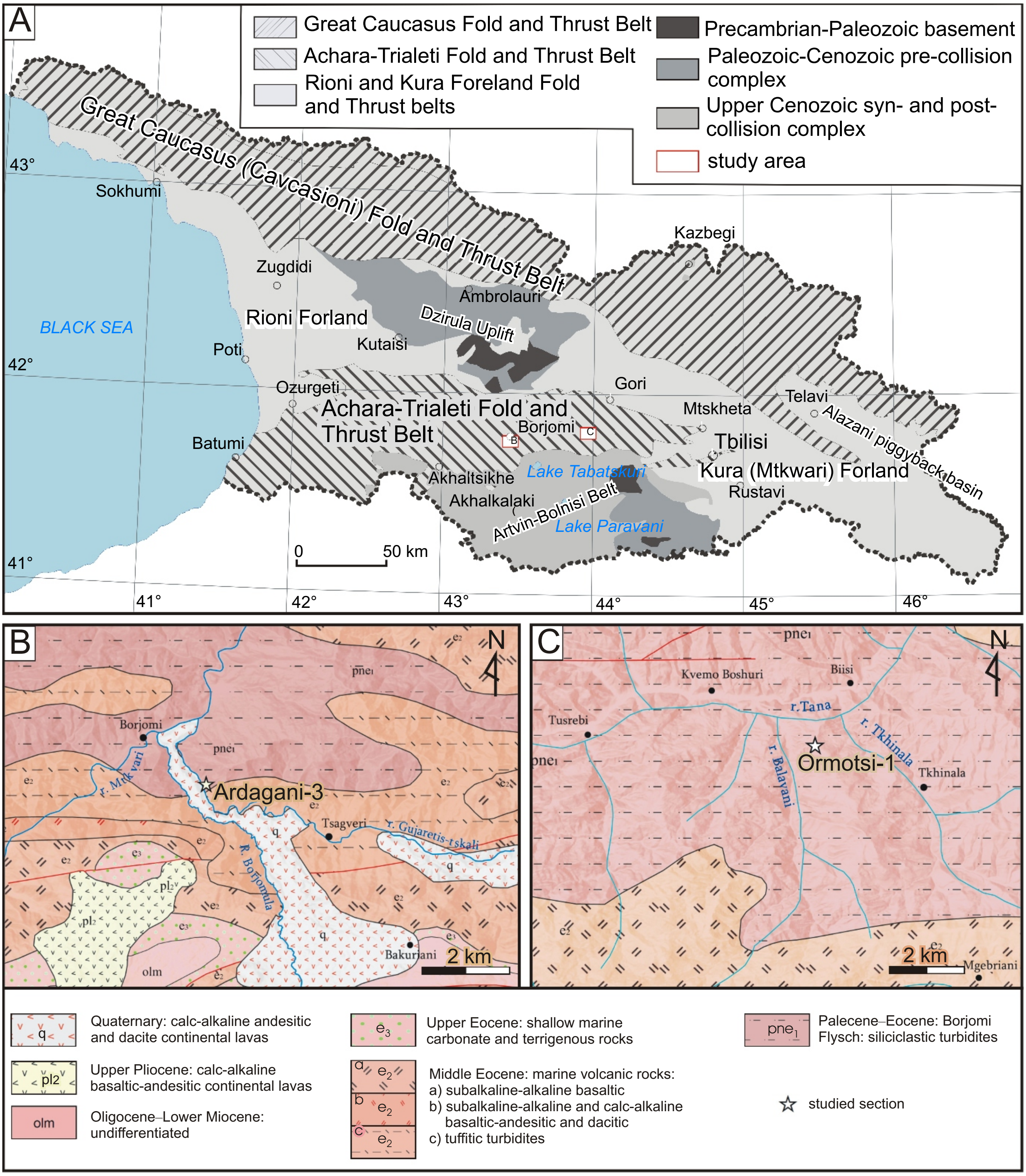

Fig. 1. Location maps

A – map of Georgia, showing the main geological units and the study area (based on Adamia et al., 2011); **B** – geological map of the Borjomi area, showing the Ardagani-3 section (based on Adamia, 2004); **C** – geological map of the river Tana Basin, showing the Ormotsi-1 section (based on Adamia, 2004)

tation toward the N or NW. Most of the mudstones and siltstones alternate with thin sandstone beds, forming packages between thicker sandstone beds. The mudstones are greenish grey or greenish without transitions, calcareous, from a few to 20 cm thick. Rarely, fresh grey mudstones form 60–70 cm thick packages. Siltstones are fairly thin, from several millimetres to 3 cm, and rare in the first 12 m of the section.

In the higher part of the section (upper part of the Boshuri Subsuite), some thick sandstone beds (40–190 cm) occur, alternating with sandstone-siltstone-mudstone packages. The

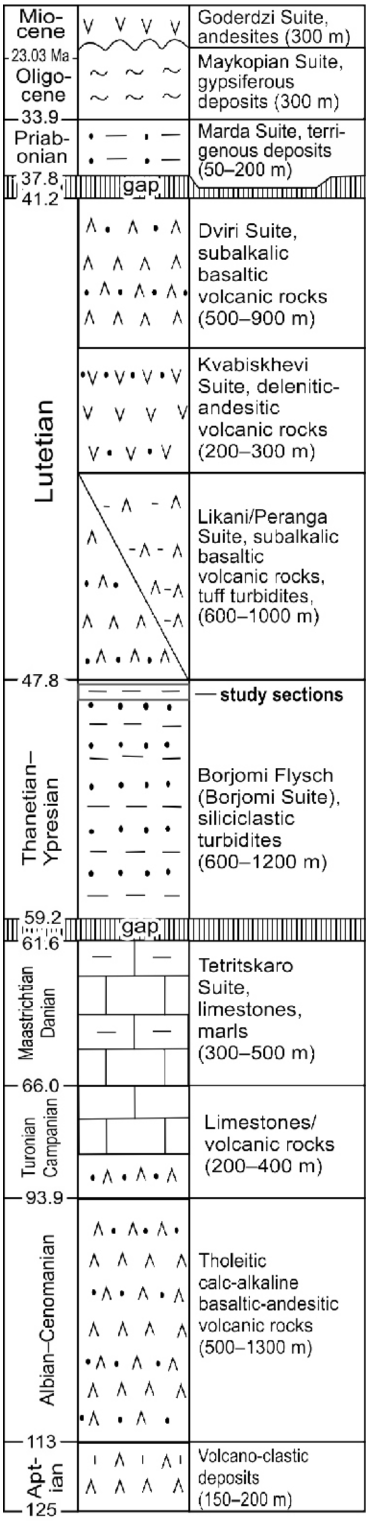

Fig. 2. Stratigraphic column of the ATFTB in the study area (based on Adamia et al., 2015, changed) showing locations of the sections studied

Dbr – debrite layer, pb – pebbles, mc – mud clasts, fc – flute casts, tb – tubular burrows, tbc – tubercles

thick beds are massive, with plant detritus at the base, and they are clearly amalgamated. Some contain mudclasts and pyritic concretions. Some thick sandstone beds are conglomeratic at the base, poorly sorted, medium to coarse grained, with abundant volcanic material. Two levels of submarine slump deposits are observed in this part of the section. The siltstone-mudstone packages were formed by one to several (up to 30, rarely more) depositional events marked by grain-size changes. Mudstone layers are thicker (from a few to 40 cm) than siltstone layers (2–3 cm).

In the Ardagani-3 section, the Bolevani Subsuite is represented by a lower shaly (41–93 m in the section) and a middle sandy unit (93–98 m in the section). The lower shaly unit consists of alternations of thin and very thin, very fine- to fine-grained sandstone beds with siltstone-mudstone intercalations arranged in 8–150 cm thick packages composed of two to 65 depositional events (heterolithic facies). In the uppermost part of the Ardagani-3 section (middle sandy unit of the Bolevani Subsuite) sandstone beds dominate and the contribution of siltstone-mudstone intercalations decreases. Plant detritus occurs at the base of some sandstone beds.

The Ardagani-3 section shows an overall thinning- and-fining-upwards trend. Deposition took place in a channelized submarine fan system, from channels on the lower slope to slope toe and encompassed various sediment gravity flows (high-and low-density turbidity currents) and hemipelagic sedimentation in a deep-sea submarine fan environment. Slumps as well as associated debrite (intervals 27.7–32.7 m; 40.03–41.33 m) and turbiditic deposits indicate instability of the slope related to extensional syn-rift tectonism and volcanic activity in the Paleogene Achara-Trialeti Basin (Beridze, 2019; Beridze et al., 2021).

The *Megagrapton aequale* studied derives from the lower shaly unit of the Bolevani (72–73 m in the section; Fig. 3) in a 3.5 cm thick, fine-grained, calcareous, mostly quartz sandstone bed amalgamated with a centimetre-thick fine-grained sandstone at the top and transitioning to 6.5 cm thick mudstone (Fig. 4). The sandstone contains small, dispersed flakes of white mica; abundant carbonized plant detritus occurs at the top of the bed. The base of the bed is sharp. It overlies light grey calcareous mudstone.

The Ormotsi-1 section (Fig. 4) is located on a dirt road, 2 km SW of the village of Biisi (~50 km east of the Ardagani-3 section), on the watershed of the Balovani and Tkhinala rivers, which are left-bank tributaries of the Tana River, in the eastern part of the ATFTB central segment (GPS coordinates: 41°51.018’N, 043°58.016’E; 1409 m a.s.l.; see Fig. 1C). The section is located in the southern limb of the Ormotsi Syncline (dip azimuth 349°, angle of dip 21°). The core of the syncline is built mainly of the Bolevani Subsuite, which is 100–150 m thick and composed of thin- and medium-bedded sandstones intercalated with mudstones and clays. Here, in contrast to the Borjomi region, the Bolevani Subsuite is not subdivided into lithological units (Papava, 1966).

The Ormotsi-1 section is nearly 3 m thick. It is composed of thin- to medium-bedded, fine- to very fine-grained, dark grey to grey sandstones intercalated with light grey to grey mudstones and rarely with clays. *Megagrapton aequale* occurs here in three fine- to medium-grained sandstone beds within a portion of the section ~1.5 m thick. The beds are 19, 7 and 5 cm thick.

ICHNOTAXONOMY

The institutional abbreviations used are as follows: GPIT-PV – Tübingen University, Germany; TSU – Department of Geology, Faculty of Exact and Natural Sciences, Iv. Javakhishvili Tbilisi State University in Tbilisi, Georgia; PIW – former collection of the Institut für Paläontologie der Universität Würzburg, now in the Bayerische Staatssammlung für Paläontologie und Geologie (SNSB) in München, Germany; TF UJ, INGUJ –

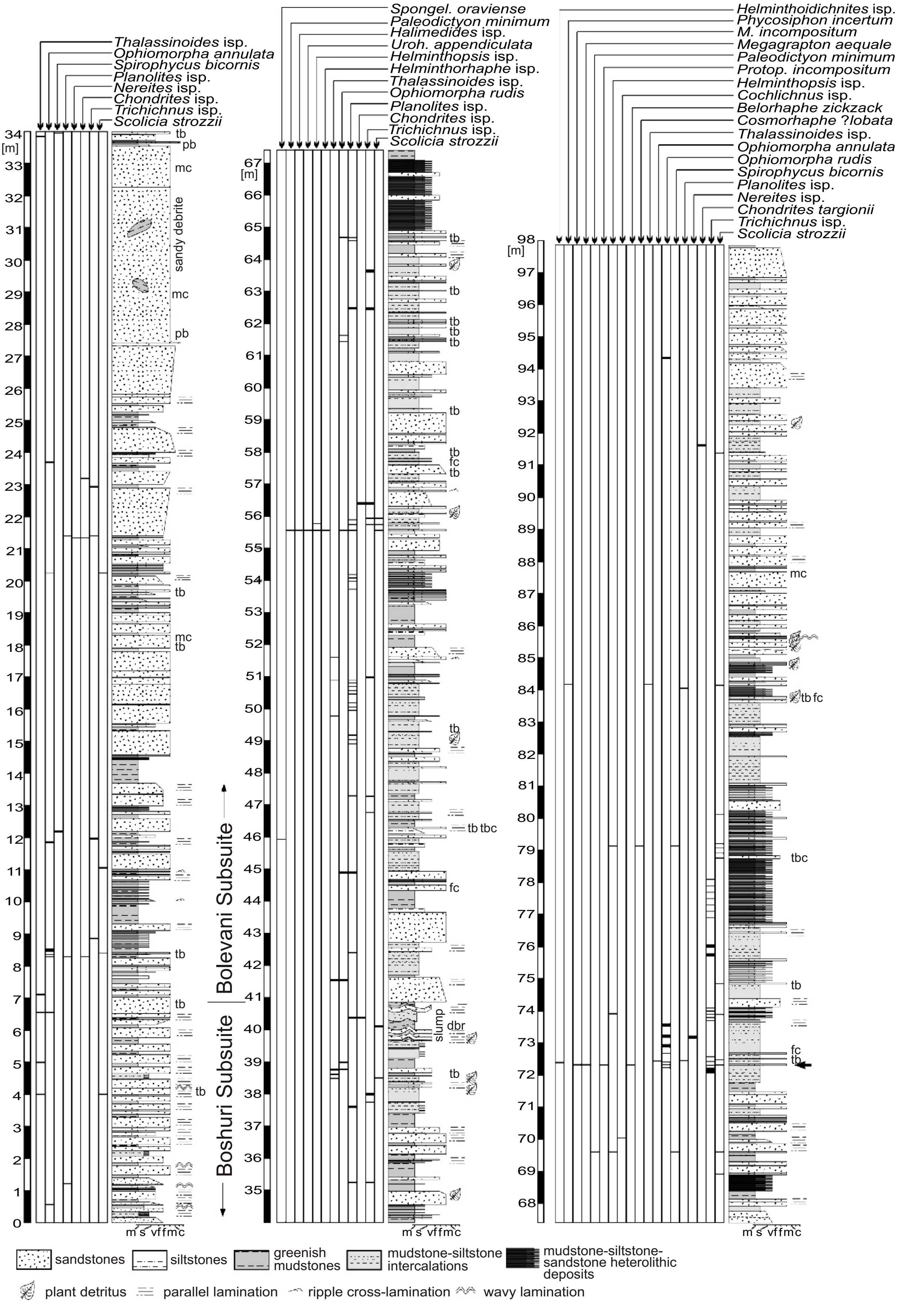

Fig. 3. The Ardagani-3 section

Arrow in the third column points to the bed with Megagrapton aequale; m – mud, s – silt, vf – very fine sand, f – fine sand, m – medium sand, c – coarse sand

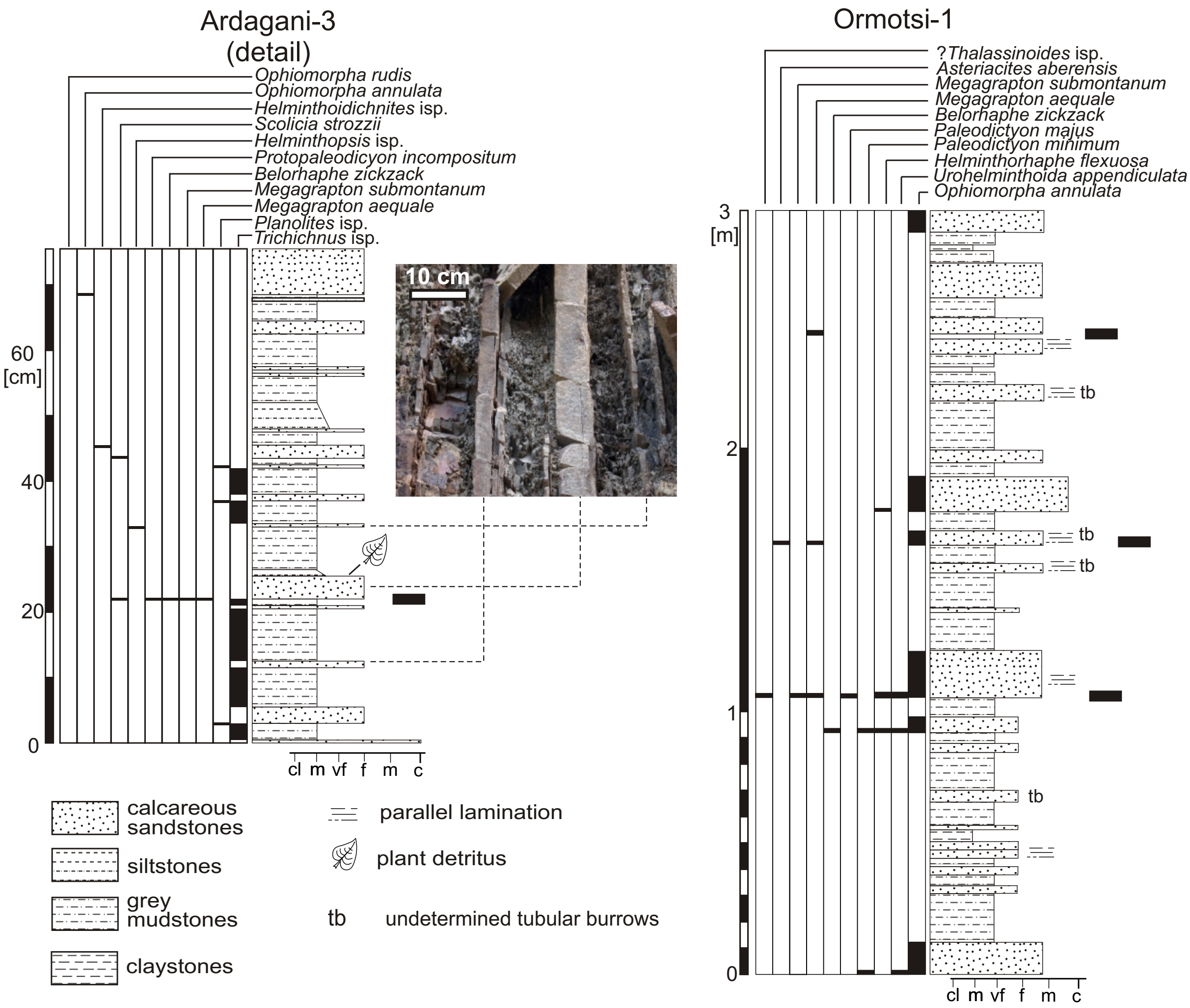

Fig. 4. Part of the Ardagani-3 section with the bed bearing *Megagrapton aequale* and the Ormotsi-1 section

Arrows indicate beds with *Megagrapton aequale;* grain-size scale: cl – clay, m – mud, vf – very fine sand, f – fine sand, m – medium sand, c – coarse sand

Nature Education Centre of the Jagiellonian University (CEP) – Museum of Geology in Kraków, Poland.

Morphometric parameters of the trace fossils considered include the maximum width of mesh (*mw*) and the width of the bordering ridge (*br*). These were measured directly on available specimens by means of an electronic caliper. Specimens from the literature and from other collections were measured from photographs by means of *ImageJ* software. Only specimens having at least one complete mesh were taken in account. The distribution of the parameters and relations between them were considered, with distinction of fields occupied by ichnospecies on plots. The coefficients of correlation (*r*) and coefficient of determination (r^2) were determined from them.

Ichnogenus *Megagrapton* Książkiewicz, 1968

T y p e i c h n o s p e c i e s. – *Megagrapton irregulare* Książkiewicz, 1968.

M o d i f i e d d i a g n o s i s. – Horizontal, branched, relatively small subcircular ridges forming irregular nets, without enlargements at the joints (modified after Uchman, 1998; Kappel, 2003).

R e m a r k s. – The diagnosis of Uchman (1998), which reads "Trace fossils commonly preserved as hypichnial irregular nets", needed to be made more precise, because some very rare but obvious *Megagrapton submontanum* from the Upper Cretaceous of Germany are preserved in full relief (Kappel, 2003) and in order to avoid having preservational aspects as the diagnostic feature. Moreover, some *Thalassinoides* or *Ophiomorpha rudis* (Książkiewicz, 1977) (see Uchman, 2009) may form horizontal, irregular meshes composed of cylindrical burrows, but these are distinctly thicker (usually 5 mm) and most of them show distinct enlargements in the joints.

Megagrapton aequale Seilacher, 1977
(Figs. 5–8)

1888 *Paleodictyon majus* Meneghini – Sacco, p. 9, pl. 1, figs. 7–10 [fig. 10 copied in Sacco, 1939, pl. 2, fig. 16].

1933 *Paleodictyon majus* Meneghini – Azpeitia Moros, p. 38, fig. 26.

non 1969 Irregular *Paleodictyon* – Simpson, p. 481, pl. 93, fig. 1 [Included in *M. aequale* by Seilacher, 1977].

?1971 *Paleodictyon maius* [sic] – Vass, p. 48, fig. 1.

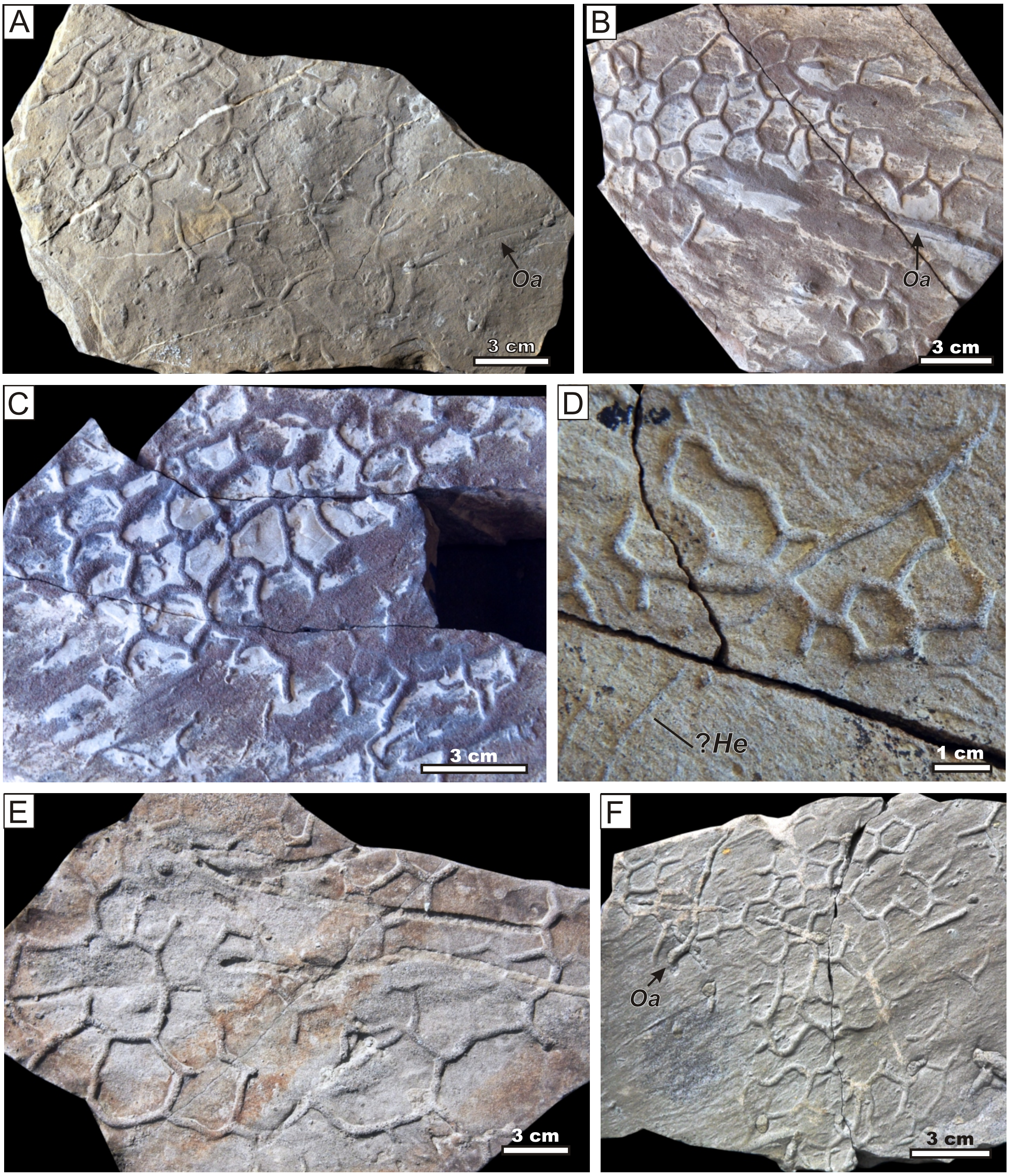

Fig. 5. *Megagrapton aequale* Seilacher, 1977; all are hypichnia on sandstone beds from Paleogene formations

A – neotype, GPIT-PV-69163 (1503-27) from Zumaya Flysch (Eocene), N Spain, housed in Tübingen University, Germany; photograph by A. Fatz; **B** – TSU01TF00001, Bolevani Subsuite (lower Eocene) of the Borjomi Flysch Ardagani-3 section, Georgia; **C** – TSU01TF00002, Bolevani Subsuite (lower Eocene) of the Borjomi Flysch, Ardagani-3 section, Georgia; **D** – TSU01TF00034, Bolevani Subsuite (lower Eocene) of the Borjomi Flysch, Ormotsi-1 section, Georgia; **E** – Monastero Formation (Oligocene), Northern Apennines, Persi 2 section, Italy, field photograph; **F** – PIW93X269, Lower Cormons Unit (Eocene), Manzano, Julian Prealps, NE Italy; *He* – *Helminthorhaphe* isp., *Oa* – *Ophiomorpha annulata*

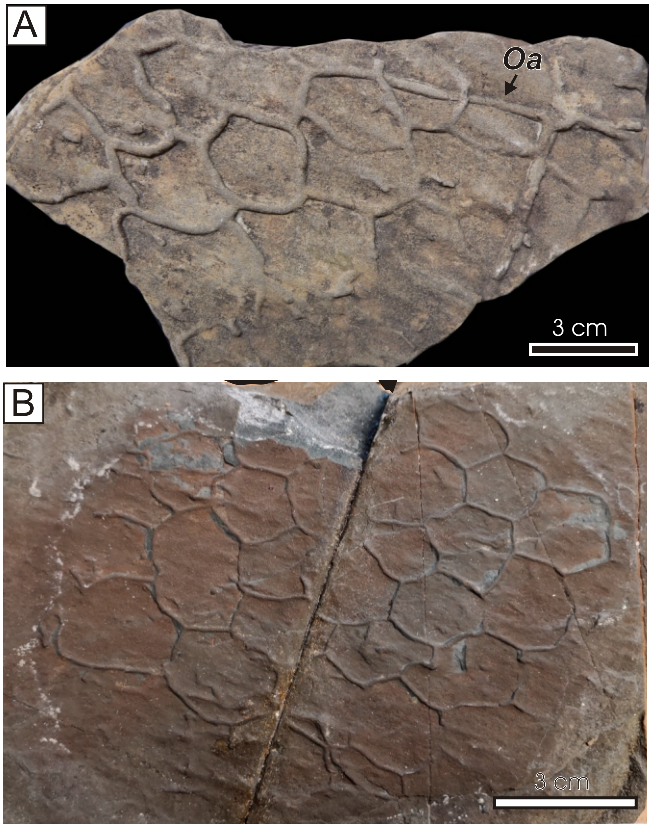

Fig. 6. *Megagrapton aequale* Seilacher, 1977

A – PIW93X422, Istria Flysch (Eocene), Boljun, Croatia; **B** – holotype of *Paleodictyon imperfectum* Seilacher, 1977 (included in *M. aequale* as *M. a. imperfectum*), specimen, 46,275, Silurian, Mull Point n. Brighouse in Kirkcudbrightshire, Scottish Uplands, UK, housed in the Cockburn Geological Museum at the Grant Institute, University of Edinburgh; photograph provided by F. Bowyer

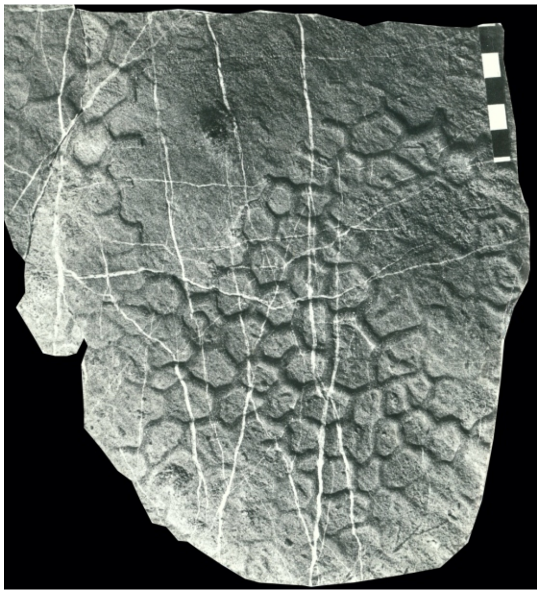

Fig. 7. *Megagrapton aequale* Seilacher, 1977 from the Szlachtowa Formation (Jurassic?, Cretaceous?), Pieniny Klippen Belt, Carpathians, Poland

This specimen was described as *Paleodictyon* by Krawczyk and Słomka (1981); photograph provided by T. Słomka

*1977 *Megagrapton aequale* n. ichnosp. – Seilacher, p. 321, fig. 11e.

1977 *Paleodictyon* (*Glenodictyum*) *imperfectum* n. ichnosp. – Seilacher, p. 325, fig. 14d, pl. 3.2.

1981 *Paleodictyon maximum* (Eichwald) – Krawczyk and Słomka, p. 68, pl. I, figs. 1 and 2, pl. 2.

1981 *Paleodictyon hexagonum* (Marck) – Krawczyk and Słomka, p. 69, pl. 2.

?1985 *Paleodictyon majus* Meneghini – Pacześna, p. 590, pl. 1, fig. 1.

1985 *Paleodictyon* isp. – Pacześna, p. 591, pl. 1, fig. 1, 2, pl. 2, fig. 1.

1985 *Paleodictyon* (*Megadictyon*) *paraimperfectum* nov. ichnosp. – Yang et Song, p. 5, pl. 1, figs. 4 and 5.

1986 *Paleodictyon* (*Glenodictyum*) *imperfectum* Seilacher – Miller, fig. 2c.

?1988 *Megagrapton aequale* – Miller, p. 367 [not illustrated].

?1992 *Megagrapton aequale* Seilacher – Kim et al., 320, fig. 3.3.

partim 1995 *Paleodictyon majus* Meneghini in de Stefani – Crimes and McCall, p. 244, fig. 6B, C.

1996 *Paleodictyon siciliense* n. ichnosp. – Kozur et al., p. 144, pl. 39, fig. 6, pl. 40, figs. 1, 4 and 7.

1996a *Paleodictyon goetzingeri* Vialov and Golev, 1965 – Tunis and Uchman, p. 183, fig. 7J, K.

1996b *Paleodictyon* (*Glenodictyum*) *arvense* Barbier – Tunis and Uchman, p. 15, fig. 14G.

1996b *Paleodictyon* (*Glenodictyum*) *croaticum* Uchman – Tunis and Uchman, p. 13, fig. 17A, D [specimen from fig. 17A shown in Marinčić et al., 1996, pl. 4, fig. 6].

1996b *Paleodictyon* (*Glenodictyum*) *goetzingeri* Vialov and Golev – Tunis and Uchman, p. 15, fig. 17B.

1996b *Paleodictyon* (*Glenodictyum*) *italicum* Vialov and Golev – Tunis and Uchman, p. 15, fig. 17C.

partim 2001 *Paleodictyon arvense* Barbier – Uchman, p. 30 [specimen PIW1998VII19].

2004 *Paleodictyon* (*Megadictyon*) *paraimperfectum* Yang et Song – Yang et al., p. 313, pl. 34, figs. 7 and 8.

partim 2016 *Paleodictyon* – Rodríguez-Tovar et al., p. 63, fig. 9C.

2014 *Paleodictyon imperfectum* – Ekdale and Gibert, fig. 3d.

partim 2016 *Paleodictyon* – Rodríguez-Tovar et al., p. 63, fig. 9C.

2018 *Paleodictyon arvense* (Barbier) – Kilibarda and Schassburger, p. 123, fig. 8G.

E m e n d e d d i a g n o s i s. – *Megagrapton* showing relatively small (in comparison to the width of the bordering ridges), variable meshes, which are mostly irregularly sub-pentagonal, sub-hexagonal or sub-heptagonal in shape and are bordered by curved or straight semicircular ridges.

H o l o t y p e. – Unfortunately, Seilacher (1977: p. 321, fig. 11e) designated a drawing (taken from a field photograph) of an uncollected specimen as the holotype of *Megagrapton aequale*. It came from the Upper Cretaceous deep-sea deposits of the Zumaya section in northern Spain. The outline of the meshes of the trace fossil illustrated by the drawing does not depart from specimens documented in this paper, but the drawing, even if

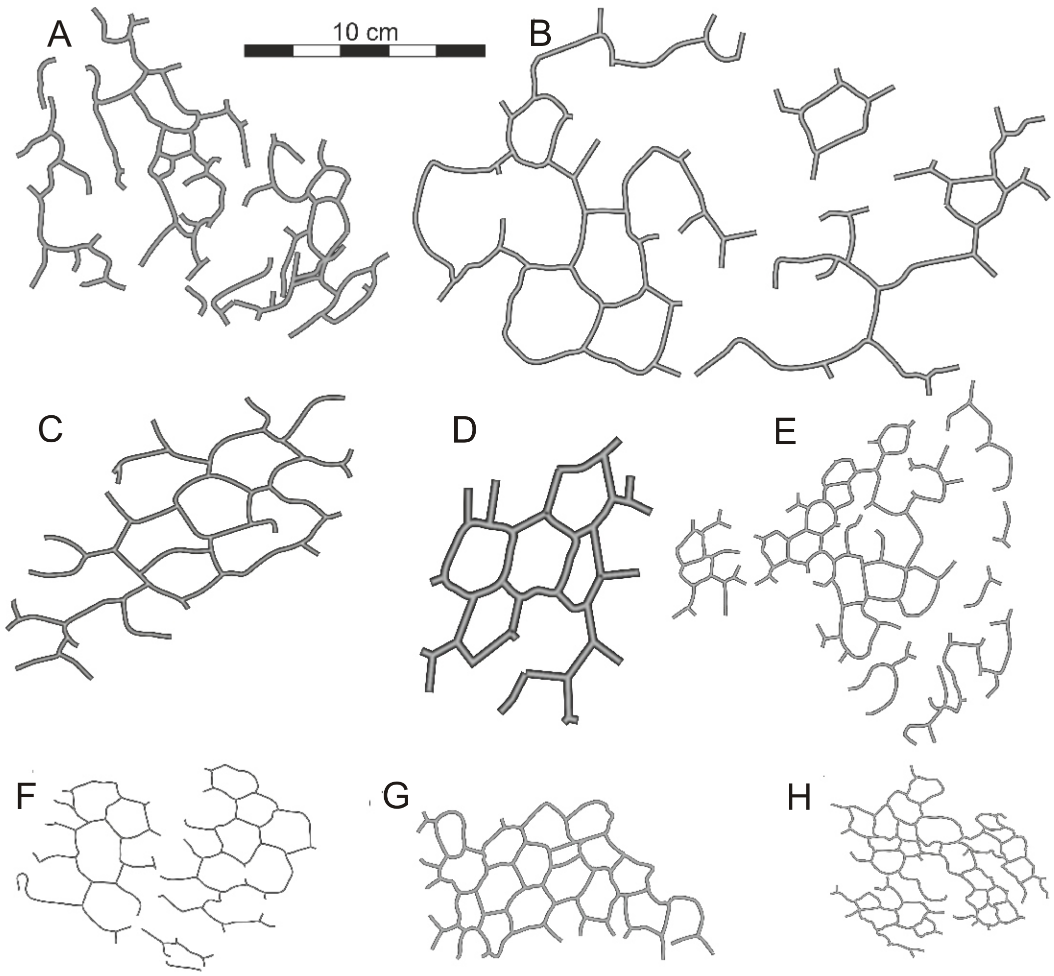

Fig. 8. Drawings of *Megagrapton aequale* Seilacher, 1977 and some ichnotaxa included within it; all are hypichnia on sandstone beds

A – neotype, GPIT-PV-69163 (1503-27) from the Zumaya Flysch (Eocene), N Spain, housed in Tübingen University, Germany (from Fig. 5A); **B** – Monastero Formation (Oligocene), Northern Apennines, Persi-2 section, Italy (based on a field photograph); **C** – PIW93X422, Istria Flysch (Eocene), Boljun, Croatia (from Fig. 6A); **D** – *Paleodictyon* (*Megadictyon*) *paraimperfectum* Yang and Song, 1985, Middle–Upper Triassic, Zhada, Ngari, Tibet, China (from Yang et al., 2004: pl. 34, fig. 7); **E** – PIW93X269, Lower Cormons Unit (Eocene), Manzano Julian Prealps, NE Italy (from Fig. 5F); **F** – holotype of *Paleodictyon imperfectum* Seilacher (now *M. a. imperfectum*), 1977, specimen, 46,275 housed in the Cockburn Geological Museum at the Grant Institute, University of Edinburgh, Silurian, Mull Point n. Brighouse in Kirkcudbrightshire, Scottish Uplands, UK (from Fig. 6B); **G** – TSU01TF00001, Bolevani Subsuite (lower Eocene) of the Borjomi Flysch, Ardagani-3 section, Georgia (from Fig. 5B); **H** – holotype of *Paleodictyon* (*Squamodictyon*) *siciliense* Kozur, Krainer and Mostler, 1996, Lercara Formation, Lower Permian, Sicily, Italy (from Kozur et al., 1996: pl. 40, fig. 7); drawings based on photographs

allowed for distinction of a new taxon/ichnotaxon by The International Code of Zoological Nomenclature (ICZN), Art. 73.1.4, is not the best choice for a holotype, especially if it is collectable. It is generally impossible to find the specimen of the holotype without determination of the exact location and in an eroded coastal cliff after half a century. Therefore, the holotype is considered to be lost. The other specimen mentioned and collected by Seilacher (1977) in the original description of *M. aequale* belongs to the type series (ICZN, Art. 72.4.1) and this is a paratype (ICZN, 72.4.5). The name-bearing type is still the holotype specimen and the illustration cannot replace it (ICZN, Art. 72.5.6). If the holotype is lost, a neotype can be selected from paratypes (ICZN, Art. 72.4.5 and Recommendation 75A). Therefore, a neotype of *M. aequale* is designated.

N e o t y p e. – GPIT-PV-69163 (1503-27), Zumaya Flysch (Eocene), northern Spain (Figs. 5A and 8A).

O t h e r m a t e r i a l. – 15 specimens TSU01TF00001-00015 from the Ardagani-3 section and 20 specimens TSU01TF00018-00037 from the Ormotsi-1 section. Bolevani Subsuite (lower Eocene) of the Borjomi Flysch.

Also material from:

– Lower Cormons Unit (lower Eocene), Julian Prealps, NE Italy, 2 specimens PIW93X269 (Manzano section); 3 specimens in Torino Museum: 17480, 17542, 17543 (all from Buttrio). For the geology and ichnology of the unit see Marincić et al. (1996) and Tunis and Uchman (1996b);
– Hecho Group (Eocene), N Spain, specimen PIW1998VII95 (Estarrún Valley, near Eposa). For the geology and ichnology of the Hecho Group see Uchman (2001), Heard and Pickering (2008) and Adserá et al. (2020);

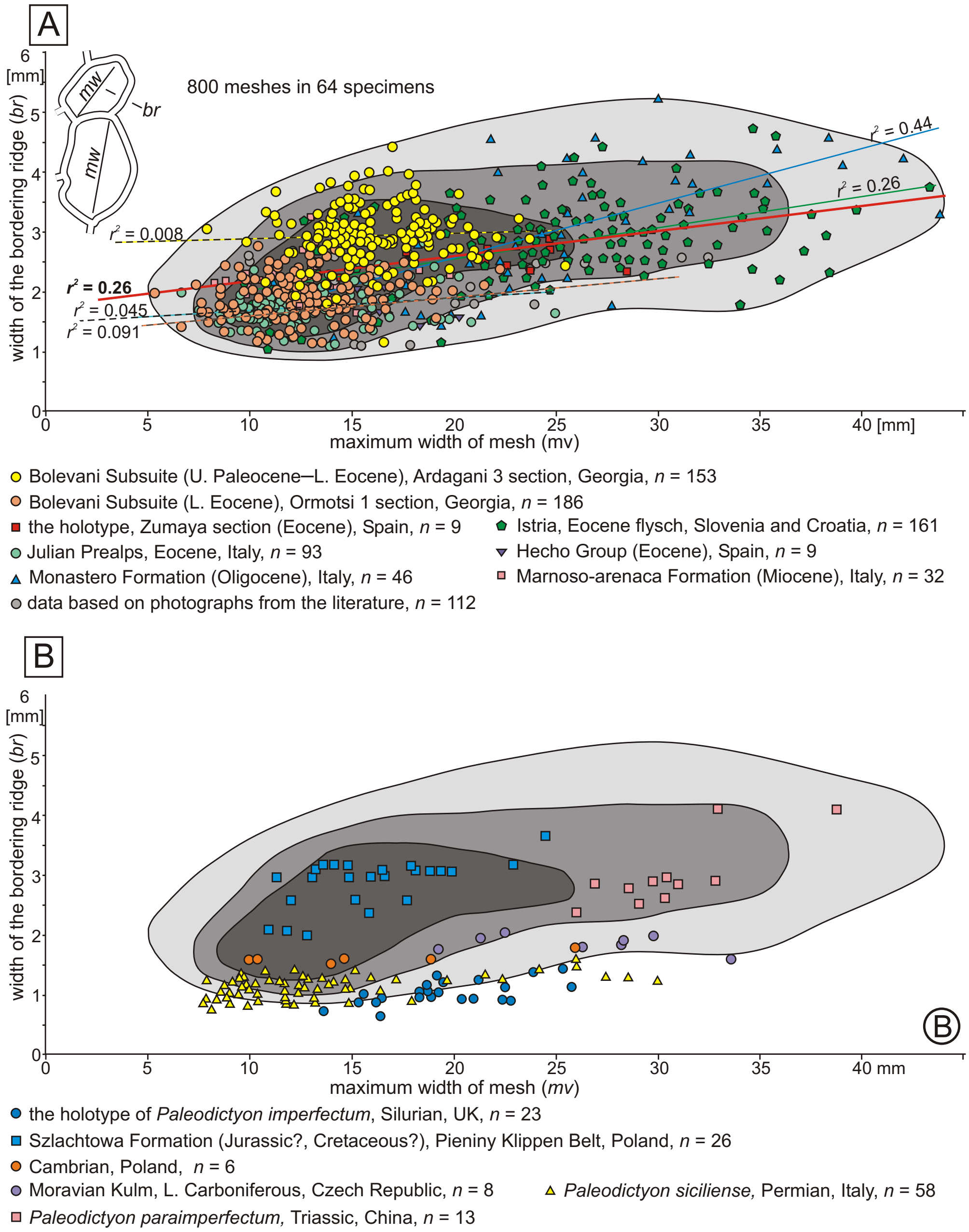

Fig. 9. Morphometric parameters of *Megagrapton aequale*

A – basic plot based on Paleogene specimens; **B** – supplementary plot showing parameters of some Paleozoic and Mesozoic specimens against the background of the plot from A; the literature data in A derive from the papers cited in the synonymy list

– Istria (Eocene), Slovenia and Croatia, 7 specimens PIW93X410, 411, 418, 422 (all from Boljun), 426 (Prodani), 429 (Senij); specimens: 5403, 5511, 6617, 6764, 6768, 6769 in the Geology Department of the Ljubljana University (all from Strunjan). For the geology and ichnology of the flysch in Istria see Tunis and Uchman (1996a);
– Marnoso-arenacea Formation (Miocene), Apennines, Italy, specimen 17539 from Torino Museum. For the geology and ichnology of the Marnoso-arenacea Formation see Uchman (1995) and Monaco et al. (2010);
– Kulm deposits (Lower Carboniferous), Czech Republic, specimen F627 (N. Těchanovice), housed in Olomouc University, Czech Republic. For the geology and ichnology of the Kulm facies in the region see Mikuláš et al. (2004).

D e s c r i p t i o n. – In positive hyporelief, the trace fossil is composed of semicircular, straight to curved, branching ridges. The ridges are smooth or with minute corrugations caused by sandstone grains. The bedding surface shows small and shallow elevations and depressions. Their elevation over the bedding surface varies on a submillimetric scale, so their width can change: the ridge becomes narrower with diminishing elevation. In places, the ridge can be slightly asymmetrical. The ridges are welded to the bedding surface, without any clear boundary, or rarely, in some parts of specimens, they are gently elevated and broken at the end, revealing their elliptical cross section.

The ridges form variable meshes, which have irregularly sub-pentagonal, sub-hexagonal or sub-heptagonal shapes. All the shapes can occur in one specimen, without any order. Individual meshes are mostly slightly elongate or rarely more or less isometric. Their longest width ranges from 5 to 15 mm. Individual meshes can have straight or curved margins depends on the course of the bordering ridges. A concave margin corresponds to a convex margin of the neighbouring mesh, and *vice versa*. None of the specimens collected show complete structure, because part of the slab is broken. Nevertheless, the number of meshes in the most complete specimens reaches about forty.

The morphometric parameters of the neotype and of other specimens from formations where they are most abundant, and the parameters of all the 688 meshes measured from 49 Paleocene–Miocene specimens, are shown in Table 1. The parameters are plotted and grouped in three different grades of density (Fig. 9A). For the highest density, the maximum mesh width ranges from 8 to 25.5 mm and the width of the bordering

Table 1

Summary of morphometric data of *Megagrapton aequale*

Section/area	*n*	*mw* [mm]		*br* [mm]		*r*	r^2
		range	mean	range	mean		
Ardagani-3, Georgia	153	7.4–26.5	16.0	0.5–4.5	3.0	0.045	0.002
Ormotsi-1, Georgia	186	5.4–22.3	12.8	1.0–3.3	1.9	0.302	0.51
Istria, Eocene flysch, Slovenia and Croatia	161	9.7–52.6	25.1	1.0–4.3	2.7	0.475	0.23
Julian Prealps, Italy	93	7.4–23.0	14.7	1.2–3.1	1.9	0.22	0.05
Monastero Formation, Italy	46	10.8–44.1	25.6	1.2–5.2	3.0	0.66	0.44
The neotype, Spain	9	14.4–28.4	22.1	2.3–2.9	2.6	0.18	0.03
All Paleocene–Miocene specimens	688	5.4–52.6	17.0	0.5–5.2	2.1	0.51	0.44

n – number of meshes measured, *mw* – maximum width of mesh, *br* – width of the bordering ridge, *r* – coefficient of correlation, r^2 – coefficient of determination

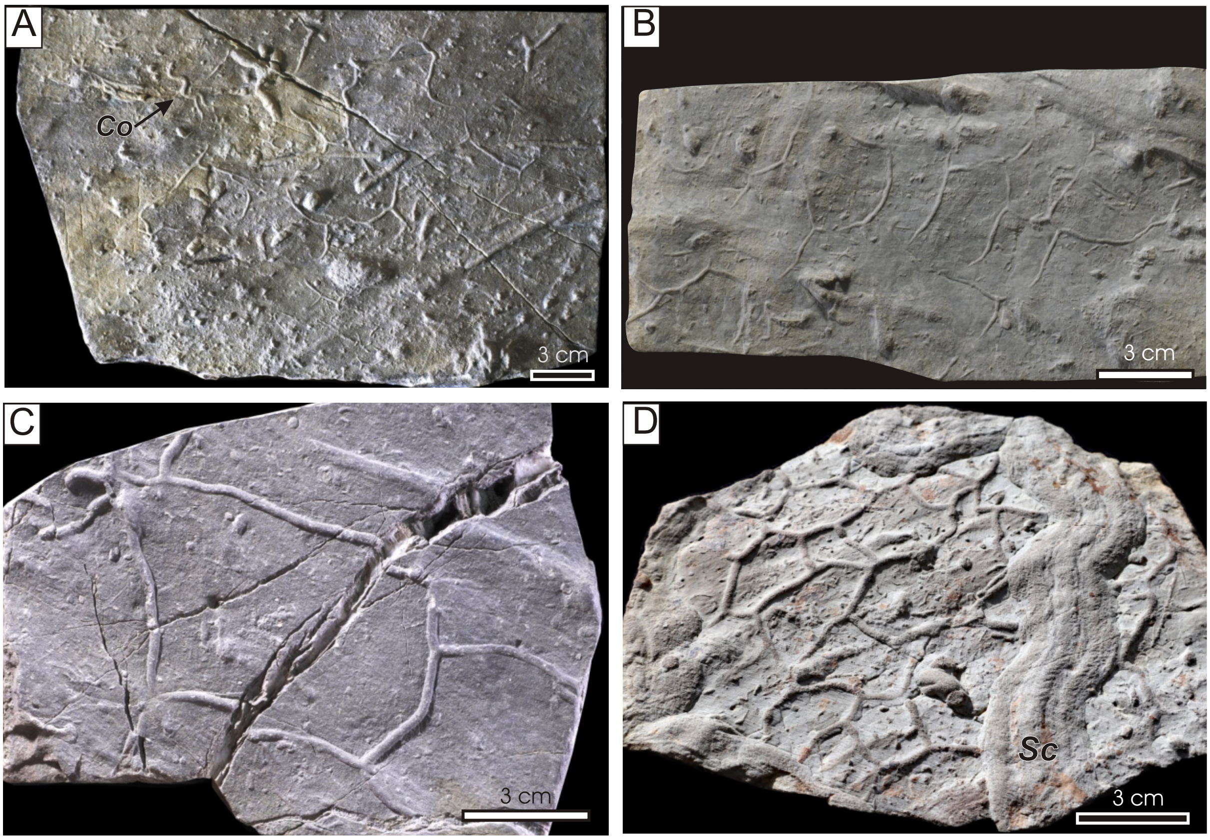

Fig. 10. *Megagrapton irregulare* Książkiewicz, 1968 and some ichnotaxa included in it

A – holotype, UJ TF 809, Beloveža Beds (Eocene), Magura Nappe, Berest, Carpathians, Poland, *Co* – *Cochlichnus* isp.; **B** – holotype of *Megagrapton tenue* Książkiewicz, 1968, UJ TF 391, Cieszyn Limestone (Berriasian), Goleszów, Carpathians, Poland; **C** – UJ TF 985, Łącko Beds (Eocene), Myślec, Magura Nappe, Carpathians, Poland; **D** – TSU01TF000016, Borjomi Suite (Paleocene–lower Eocene), Satovle, Georgia; *Sc* – *Scolicia* isp.

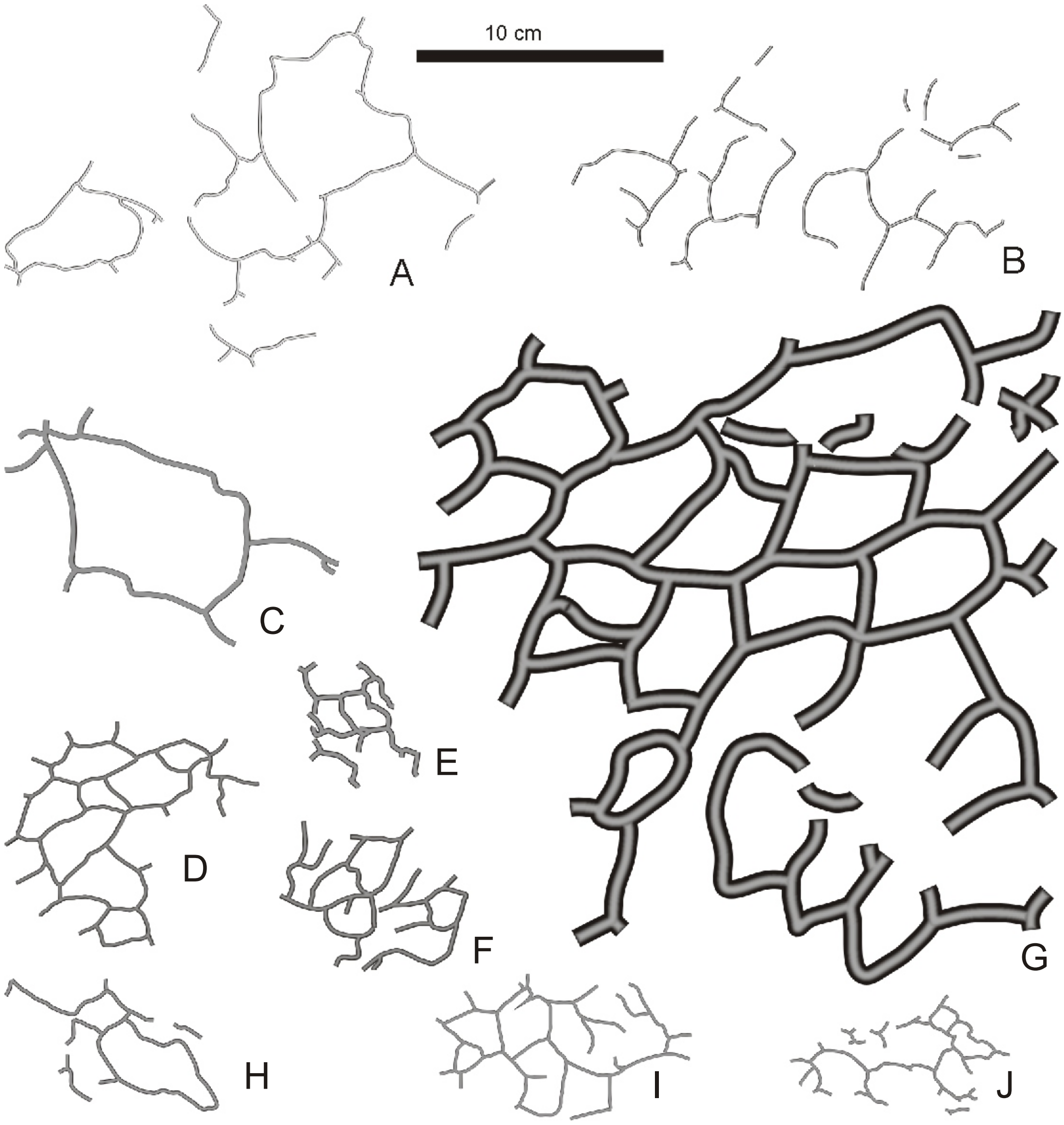

Fig. 11. Drawings of *Megagrapton irregulare* Książkiewicz, 1968 and some ichnotaxa included within it; all are hypichnia on sandstone beds

A – holotype, UJ TF 809, Beloveža Beds (Eocene), Magura Nappe, Berest, Carpathians, Poland (from Fig. 10A); **B** – holotype of *Megagrapton tenue* Książkiewicz, 1968, UJ TF 391, Cieszyn Limestone (Berriasian), Goleszów, Carpathians, Poland (from Fig. 10B); **C** – UJ TF 985, Łącko Beds (Eocene), Myślec, Magura Nappe, Carpathians, Poland (from Fig. 10C); **D** – TSU01TF000016, Borjomi Suite (Paleocene–lower Eocene), Satovle, Georgia (from Fig. 10D); **E** – holotype of *Megagrapton angulare* Stepanek and Geyer, 1989 (from Stepanek and Geyer, 1989: pl. 3, fig. 24); **F** – *Paleodictyon* (*Megadictyon*) *wuhaiensis* Yang, Zhang and Yang, 2004, Middle Ordovician, Wuhai, Inner Mongolia, China, (from Yang et al., 2004: pl. 34, fig. 5); **G** – *Irredictyon chaos* Vialov, 1972 (now *M. i. chaos*), Paleogene of Dagestan (from Vialov, 1972: pl. 3); **H** – holotype of *Megagrapton permicum* Kozur, Krainer and Mostler, 1996, Lercara Formation, Lower Permian, Sicily, Italy (from Kozur et al., 1996: pl. 39, fig. 2); **I** – holotype of *Paleodictyon* (*Megadictyon*) *muelleri* Kozur et al., 1996, Lercara Formation, Lower Permian, Sicily, Italy (from Kozur et al., 1996: pl. 39, fig. 7); **J** – holotype of *Megagrapton transitum* Kozur et al., 1996, Lercara Formation (Lower Permian), Sicily, Italy (from Kozur et al., 1996: pl. 39, fig. 1); drawing based on photographs

ridges ranges from 1.5 to 3.5 mm. Parameters from the sections and formations overlap but differ more or less distinctly. Parameters of specimens from older formations are plotted also (Fig. 9B). Some of these overlap well with the main field but some only partly. Nevertheless, the outline of their meshes is basically the same (Figs. 7 and 8D, F, H).

R e m a r k s. – The original diagnosis by Seilacher (1977: 321) reads: "Majority of second order undulations anastomosing. The meshes are rather narrow and uniform in size, but without uniform shape or orientation". However, as it is unclear what the first- or second-order undulations are in the trace fossil discussed, a new diagnosis is proposed that focuses on the morphology of the meshes and the course of the bordering ridges.

Aside from the specimen assigned in this paper as the neotype, Seilacher (1977) pointed to a specimen presented by Simpson (1969: pl. 93, fig. 1) as an example of *Megagrapton aequale*, but this was included in *M. irregulare* Książkiewicz

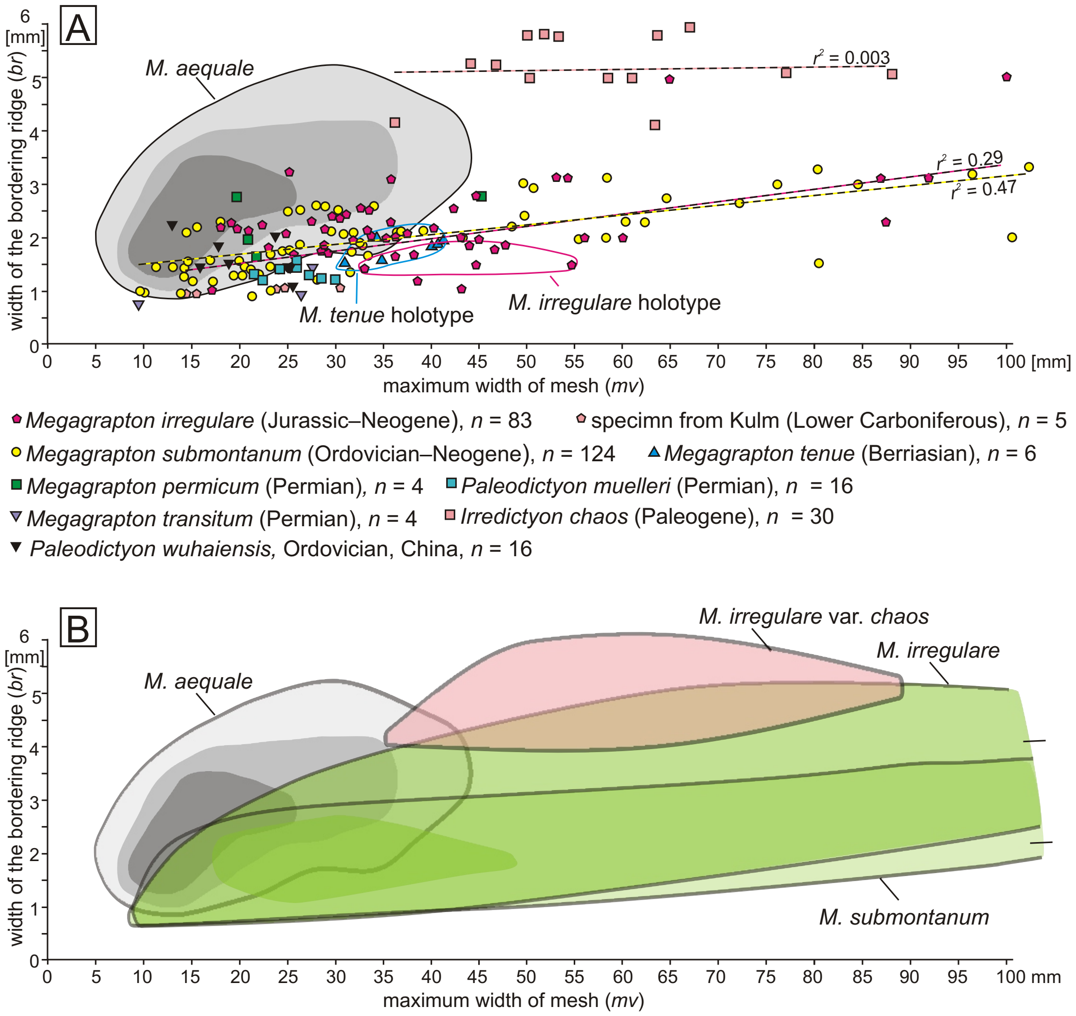

Fig. 12. Morphometric parameters of *Megagrapton irregulare* Książkiewicz, 1968 and *M. submontanum* (Azpeitia Moros, 1933) for specimens in which the width of meshes is less than 100 mm

A – plot of data against the background of *M. aequale*;
B – ichnospecies of *Megagrapton* – delineation of main fields of morphometric parameters

(Uchman, 1998). A new inspection of this specimen has revealed that it shows the features of *M. submontanum.*

After its establishment, *Megagrapton aequale* was very rarely used in the literature (two citations in the synonymy and occurrence list), mainly because it was mistaken for *Paleodictyon*. The survey of literature and collections reveals that *M. aequale* is confused with and included in other ichnotaxa, especially *Paleodictyon* Meneghini in Savi and Meneghini, 1850, including the type material of some ichnospecies. Besides the outline of meshes described in the diagnosis, their morphometric parameters overlap entirely or partly with the field occupied by the Paleogene material (Fig. 9B). These ichnospecies include *Paleodictyon imperfectum* Seilacher, 1977 (holotype from the Silurian of Mull Point in the vicinity of Brighouse in Kirkcudbrightshire, Scottish Uplands, Figs. 6B and 8F) and *Paleodictyon siciliense* Kozur, Mostler and Krainer, 1996 (holotype from the Permian of Sicily, Italy, Fig. 8H). The only difference is that the width of the bordering ridge in their holotypes is generally narrower than in Paleogene *M. aequale* (Fig. 9B). Moreover, *P.* (*Megadictyon*) *paraimperfectum* Yang and Song, 1985 (type material from Middle–Upper Triassic of Tibet; Fig. 8D) is also included in *M. aequale*. Although these three ichnospecies are included in *M. aequale*, their variability is poorly known because their type material is poorly represented. In the current state of knowledge, the ichnosubspecies *Megagrapton aequale imperfectum* (Seilacher, 1977) comb. nov. is proposed. *Paleodictyon siciliense* Kozuret al., 1996 belongs to it. This variety is characterized by a relatively thin bordering ridge, with a width of 1 mm.

Megagrapton aequale ranges from the lower Cambrian (Pacześna, 1985; see the synonymy and occurrence list) to the upper Miocene (Ekdale and Gibert, 2014). Its most common occurrences are in Paleogene strata. *Megagrapton aequale* occurs almost exclusively in deep-sea turbiditic deposits. The depositional environment of the lower Cambrian occurrence is still poorly understood. In the Ardagani-3 section, *M. aequale* co-occurs *with M. submontanum, Protopaleodictyon incompositum*, *Belorhaphe zickzack, Scolicia strozzii,* and *Ophiomorpha rudis* in the same bed, and with *Trichichnus* isp., *Planolites* isp., *Scolicia strozzii, Helminthopsis* isp., *Helminthoidichnites* isp., and *Ophiomorpha annulata* in the interval from one metre below the bed with *M. aequale* to one metre above it (Fig. 4). In the Ormotsi-1 section, *M. aequale* co-occurs with *O. annulata, Helminthorhaphe flexuosa, Urohelminthoida appendiculata*, *M.*

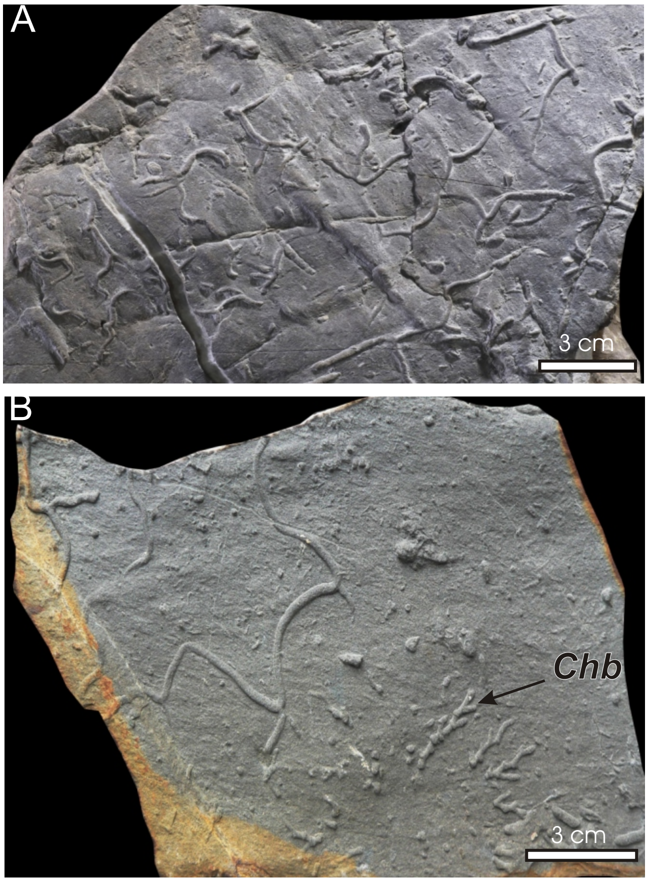

Fig. 13. *Megagrapton submontanum* (Azpeitia Moros, 1933)

A – UJ TF 388, Beloveža Beds, Eocene, Magura Nappe, Lipnica Mała, Carpathians, Poland; **B** – PIW93X243, Flysch del Grivó, Paleocene–Eocene, Anhovo, Julian Prealps, Slovenia; *Chb* – *Chondrorhaphe bifida*

submontanum, *Paleodictyon majus, Asteriacites quinquefolius,* and ?*Thalassinoides* isp. in the same beds. Moreover, *Belorhaphe zickzack* and *Paleodictyon minimum occur in a neighbouring bed* (Fig. 4).

Megagrapton irregulare Książkiewicz, 1968
(Figs. 10–12)

v* 1968 *Megagrapton irregulare* n. "sp." – Książkiewicz, p. 5, text-fig. 3.

v 1968 *Megagrapton tenue* n. "sp." – Książkiewicz, p. 5, pl. 3, fig. 1.

non 1988 *Megagrapton irregulare* – Pickerill et al., p. 142, fig. 2e [epichnion].

1972 *Irredictyon chaos* sp. n. – Vialov, p. 79, pl. 3, fig. 1, pl. 4, figs. 1 and 2.

? 1998 *Megagrapton irregulare* Książkiewicz – Schweigert, p. 15, fig. 4.

1996 *Megagrapton permicum* n. ichnosp. – Kozur et al., 1996, p. 138, pl. 39, fig. 2, pl. 40, figs. 2, 5 and 6.

1996 *Paleodictyon* (*Megadictyon*) *muelleri* n. ichnosp. – Kozur et al., p. 145, pl. 39, fig. 7.

1996 *Megagrapton transitum* n. ichnosp. – Kozur et al., p. 140, pl. 39, figs. 1 and 5, pl. 41, fig. 2.

2004 *Paleodictyon* (*Megadictyon*) *wuhaiensis* ichnosp. nov. – Yang et al., p. 313, pl. 34, fig. 5.

2003 *Megagrapton irregulare* Książkiewicz – Kappel, p. 93, text-fig. 11.13.1, pl. 12, figs. 2–5.

v 2005 *Megagrapton irregulare* Książkiewicz – Uchman et al., p. 124, fig. 20A.

2007 *Megagrapton irregulare* – Wetzel et al., p. 571, a part of fig. 6.

2009 *Megagrapton irregulare* Książkiewicz – Warchoł and Leszczyński, p. 9, fig. 10.

? 2010 *Megagrapton* cf. *irregulare* – Monaco et al., pl. 3, fig. 4.

v 2012 *Megagrapton irregulare* Książkiewicz – Uchman and Wetzel, 645, fig. 1D.

non 2015 *Megagrapton irregulare* Książkiewicz – Khaidem et al., p. 1094, fig. 5a.

? 2015 *Megagrapton irregulare* – Zayats et al., p. 83, fig. 3.

?non 2019 *Megagrapton irregulare* Książkiewicz – Luo et al., p. 12, p. 4G.

non 2021 *Megagrapton irregulare* Książkiewicz – Sabhaya et al., p. 45, fig. 2d [*Thalassinoides* isp.]

H o l o t y p e. – UJ TF 809, Beloveža Beds (Eocene), Berest, Carpathians, Poland (Figs. 11A and 12A).

D i a g n o s i s. – *Megagrapton* with meshes bordered by mostly slightly winding ridges, which commonly branch at approximately right angles (modified after Uchman, 1998).

R e m a r k s. – In the diagnosis the word "mostly" replaces the word "only" and the word "ridges" replaces "strings" in the emended diagnosis by Uchman (1998). This is because some bordering ridges (the term "ridge" better expresses the morphology than the term "string") in *Megagrapton irregulare* can be strongly winding, as in *M. submontanum*.

The synonymy and occurrence list completes that of Uchman (1998). The holotypes of *Megagrapton permicum* Kozur et al., 1996 (Fig. 11H), *Paleodictyon* (*Megadictyon*) *muelleri* Kozur et al., 1996 (Fig. 11I), and *M. transitum* Kozur et al., 1996 (Fig. 11J), all from the Lower Permian Lercara Formation of Sicily in Italy, and *P. (M.) wuhaiensis* Yang et al., 2004 (the type material from the Middle Ordovician, China, Fig. 11F) display the diagnostic features of *M. irregulare* and are included in the list. It is proposed that *M. tenue* Książkiewicz, 1968 (Figs. 11B and 12B) is a synonym of *M. irregulare* (see Uchman, 1998) on the same basis.

The plot of morphometric parameters of *Megagrapton irregulare* shows that that most of the maximum widths of meshes range from 15 to 50 mm, and the thickness of the bordering ridges from 1 to 2.5 mm (Fig. 12A). However, there are also rare specimens with very large meshes, >100 mm wide.

Irredictyon chaos Vialov, 1972 (Fig. 12G) from the Paleogene of Dagestan (Caucasus region) shows meshes whose overall shape is like those in *M. irregulare* but with much thicker bordering ridges, and its morphometric parameters are outside of the morphometric parameters of *M. irregulare* (Fig. 13A). Unfortunately, it is known to us only from a few photographs. Häntzschel (1975: W74) commented on it as "similar to *Paleodictyon,* but meshwork of burrows more irregular". Uchman (1998) included it in *M. irregulare*. This is followed in this paper, but this trace fossil can be distinguished as the ichnosubspecies *M. irregulare chaos* (Vialov, 1972) comb. nov. because of the very thick bordering ridges.

Megagrapton irregulare ranges from the Ordovician (Uchman et al., 2005) to the Miocene (D'Alessandro, 1981). It occurs mostly in deep-sea turbiditic deposits.

Megagrapton submontanum (Azpeitia Moros, 1933)
(Figs. 13–15)

*1933 *Cylindrites submontanus* n. sp. – Azpeitia Moros, p. 44, fig. 21b.

v 1961 *Palaeochorda submontana* (Azpeitia) – Książkiewicz, 883, pl. 1, fig. 3.

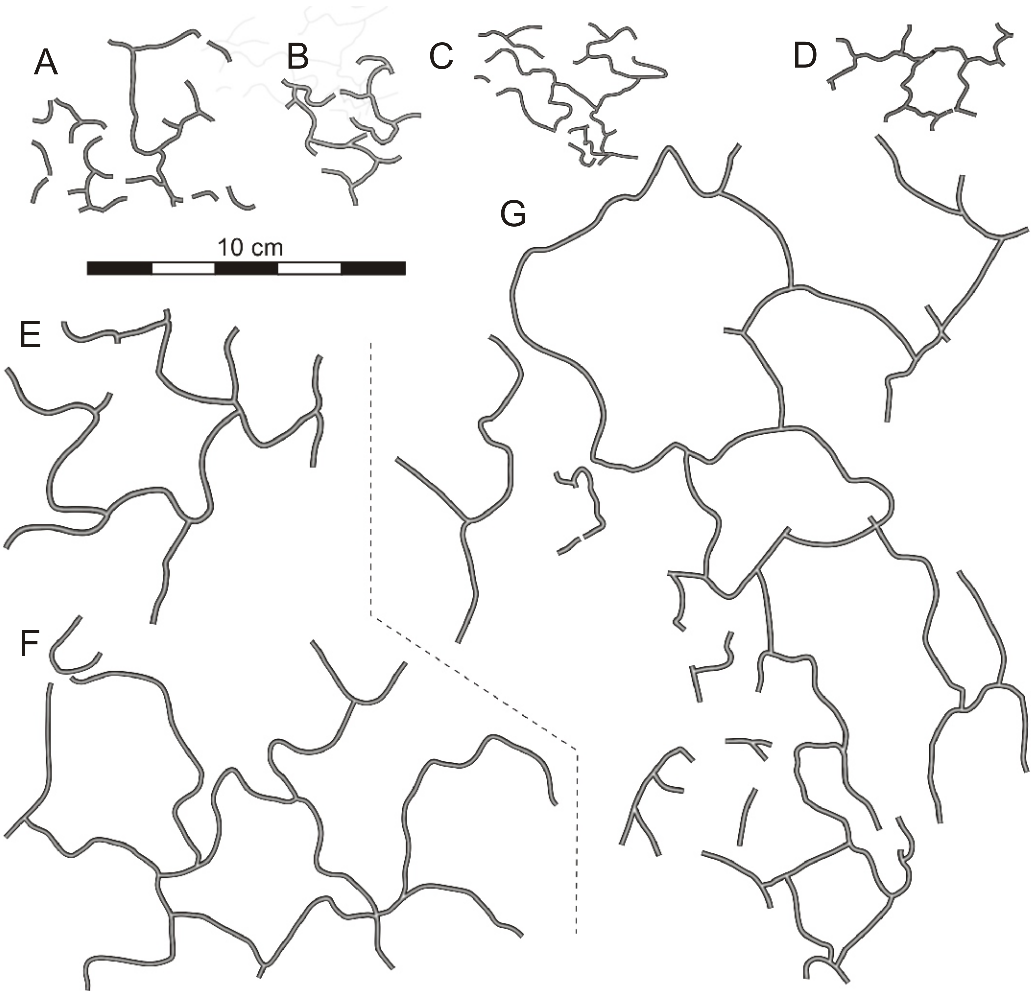

Fig. 14. Drawings of *Megagrapton submontanum* (Azpeitia Moros, 1933) redrawn from photographs; all are hypichnia on sandstone beds

A – holotype, Eocene, Zumaya, N. Spain (from Azpeitia Moros, 1933, fig. 21b); **B** – INGUJ144P241, Hieroglyphic Beds, Eocene, Magura Nappe, Grzechynia, Carpathians, Poland, coll. W. Grabowski; **C** – UJ TF 1255, Magura Nappe, Beloveža Beds, Eocene, Lipnica Mała, Carpathians, Poland; **D** – Hecho Group (Eocene), Pyrenees, N Spain (from Uchman, 2001: pl. 13, fig. 1); **E** – INGUJ144P242, Beloveža Beds (Eocene), Magura Nappe, Kamionka Wielka, Carpathians, Poland, coll. M. Kasprzyk; **F** – Ganei, Eocene, Swiss Alps (from Wetzel and Uchman, 1997: fig. 5E); **G** – Howin Group, Ordovician, Fettenfjord B, Norway (from Uchman et al., 2005: fig. 20B)

1967 *Unarites suleki* sp. n. – Macsotay, 38, figs. 27, 29 and 36.

v partim 1977 *Protopaleodictyon submontanum* (Azpeitia) – Książkiewicz, 177, pl. 25, figs. 1, 2, 4 and 5, text-fig. 41b–n, p [non pl. 25, fig. 3, text-fig. 41a, o = *Megagrapton irregulare*].

1998 *Megagrapton submontanum* (Azpeitia Moros) – Uchman, p. 194, fig. 105A–C.

2001 *Megagrapton submontanum* (Azpeitia Moros) – Buatois et al., p. 48, figs. 8.2, 8.7.

2003 *Megagrapton submontanum* (Azpeitia Moros) – Kappel., p. 94, pl. 10, fig. 4, pl. 11, fig. 2.

v 2005 *Megagrapton irregulare* Książkiewicz – Uchman et al., p. 125, fig. 20B.

? 2008 *Megagrapton submontanum* (Azpeitia Moros) – Zhang et al., p. 53, figs. 6a, c, 7f.

2008 *Megagrapton submontanum (*Azpeitia-Moros, 1933) – López Cabrera et al., 383, fig. 4.2

2010 *Megagrapton submontanum* – Nielsen et al., 2010, p. 696, fig. 5, E, F.

v 2010 *Megagrapton submontanum* – Rodríguez-Tovar et al., p. 58, fig. 6a.

? 2014 *Megagrapton submontanum* – López Cabrera and Olivero, p. 35, fig. 2c.

? 2014 *Megagrapton* – Monaco and Trecci, p. 121, pl. 2C.

2020 *Megagrapton submontanum* – Demircan and Görmüş, p. 485, fig. 19E.

2021 *Megagrapton irregulare* Książkiewicz – Madon, p. 38, fig. 15E.

H o l o t y p e. – A specimen illustrated by Azpeitia Moros (1933: fig. 21b; Fig. 14A) from the deep-sea Eocene of Zumaya in N Spain, found in the collection of trace fossils described by Azpeitia Moros in the Geominero Museum of the Geological Survey of Spain in Madrid (information from the museum in 2021).

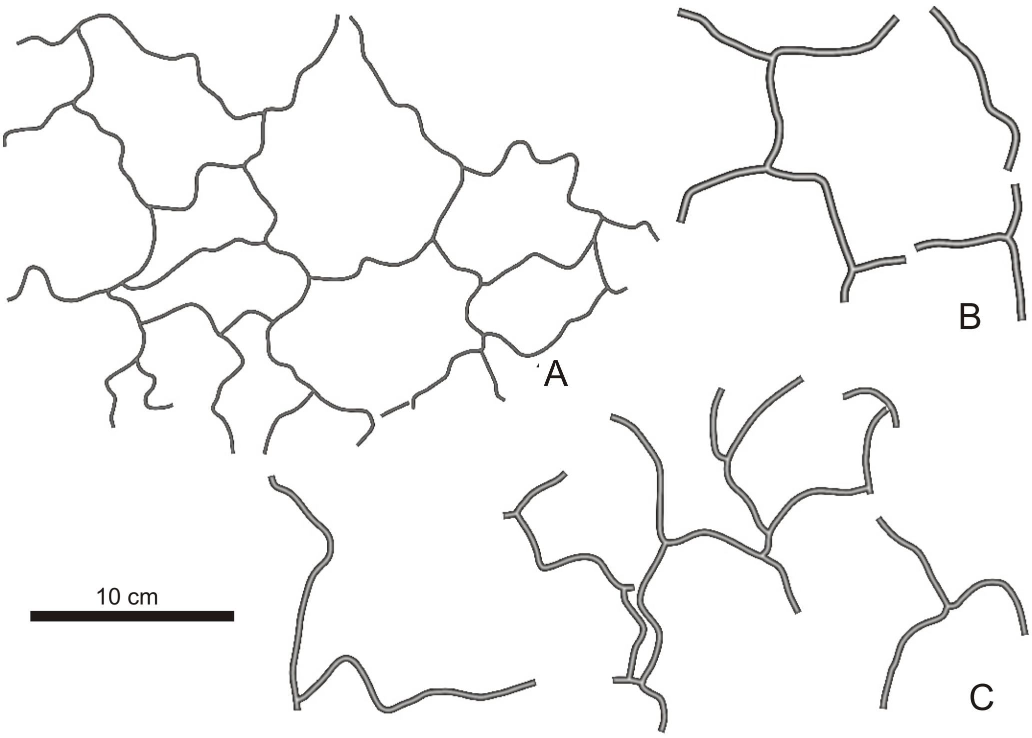

Fig. 15. Drawings of very large *Megagrapton*

A – *M. submontanum,* Spain (from Rodríguez-Tovar et al., 2016: fig. 9A); **B** – *M. ?submontanum,* INGUJ144P228, Ropianka Formation (Campanian–Paleocene), Magura Nappe, Zamieście, Carpathians, Poland; **C** – *M. submontanum,* Beloveža Beds, Eocene, Magura Nappe, Zbludza, Carpathians, Poland

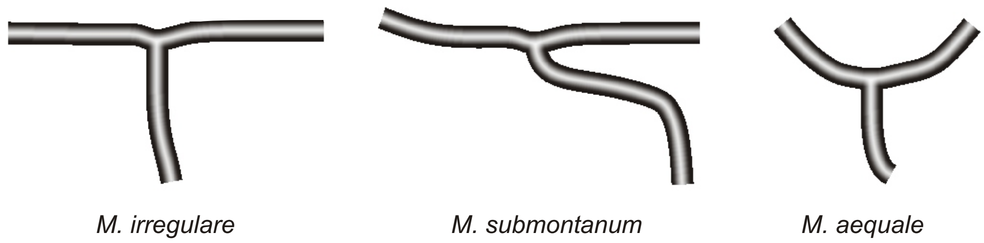

Fig. 16. Characteristic types of branching in ichnospecies of *Megagrapton*

D i a g n o s i s. – *Megagrapton* with meshes bordered mostly by distinctly winding bordering ridges. Acute angles of branching are common (modified by Uchman, 1998).

R e m a r k s. – The word "mostly" is added to the diagnosis by Uchman (1998) to underscore that the winding bordering ridges ("strings" in the former diagnosis) are not present in every mesh.

The synonymy and occurrence list provided completes that of Uchman (1998). This ichnospecies was originally described under *Cylindrites* Göppert, 1842, later under *Palaeochorda* M Coy in Sedgwick, 1848, *Protopaleodictyon* Książkiewicz, 1958, and finally under *Megagrapton* Książkiewicz, 1960. *Unarites suleki* Macsotay, 1967 from the Paleocene of Venezuela is considered as its junior synonym (Uchman, 1998). *Unarites tibetus* Yang and Song, 1985 (pl. 2, fig. 3) from the Triassic of Tibet shows loops rather than meshes. Its only photograph was reproduced in Yang et al. (2004: pl. 26, fig. 2) as *Megagrapton tibeticum;* however, Yang and Song (1985) distinguished *Megagrapton tibeticum* as a new ichnospecies on the basis of other specimens (their pl. 2, fig. 3).

A plot of morphometric parameters of *Megagrapton submontanum* shows a similar trend to that of *M. irregulare*. There is a slight tendency for the smallest meshes in *M. submontanum* to be smaller than in *M. irregulare* and the bordering ridges are slightly thinner. The meshes of some rare specimens are very large, with widths exceeding 100 mm (Fig. 15).

Megagrapton submontanum ranges from the Ordovician (Uchman et al., 2005) to the lower Miocene (López Cabrera et al., 2008). It occurs in deep-sea turbiditic deposits.

DISCUSSION

Megagrapton and related trace fossils are interpreted as a system of shallow, horizontal, branched tunnels within the sediment. *Megagrapton* Książkiewicz, 1968 may be distinguished from *Pseudopaleodictyon* Pfeifer, 1968, typified by *P. hartungi* (Geinitz, 1867), and *Multina* Orłowski, 1968, typified by *Multina magna* Orłowski, 1968, because in the latter two the bordering ridges or tunnels commonly show overcrossings (Uchman, 1998). They are preserved in full relief, not rarely at the top or inside the beds, and the ridges or tunnels run more frequently at different levels in *Pseudopaleodictyon* and *Multina*, but this criterion is equivocal because some specimens of *Megagrapton* also show some tunnels departing from one level. Some of them run gradually above the bedding level and are preserved in full relief in short segments. Thus, a transition from semirelief to full relief can be observed.

Megagrapton fornicatum Kappel, 2003 from the Upper Cretaceous of Germany (Kappel, 2003: p. 94, text-fig. 11.13.2, pl. 12, figs. 1 and 6) is excluded from this ichnogenus. *M. fornicatum* shows very small, very irregular meshes (2–23 mm wide), and bordering ridges that show overcrossings. This trace fossil fits better to *Multina*.

Megagrapton tibeticum Yang and Song, 1985 from the Triassic of Tibet (their pl. 2, fig. 2), shows two (?) poorly preserved meshes and it is hard to assess its distinctiveness from or affinity with other ichnospecies of *Megagrapton* and whether it belongs to *Megagrapton* at all. *M. fupingensis* Yang et al., 2004, from the Upper Ordovician of China (Yang et al., 2004: p. 167, pl. 26, figs. 3–5), shows several overcrossings of winding ridges and occasional doubtful meshes. It is not clear if this is *Megagrapton* in the sense of the current diagnosis. *M. regulare* Ghare and Badve, 1977 (their pl. 7, fig. 2), from the Kimur Series (Vindhayan, Mezoproterozoic) of India, which is composed of furrows forming subquadrate polygons is a physical structure, probably a network of filled fissures on a bedding surface. Wilson et al. (2021) described pyritized burrows from the Devonian black shales of North America, which are composed of irregular meshes with nodes (?); these were determined as “very similar to the ichnogenus *Megagrapton*”. However, they are located in several adjacent levels and resemble more *Multina* than *Megagrapton*.

Three ichnospecies of *Megagrapton* are recommended for further use: *M. irregulare* as the type ichnospecies, *M. aequale* and *M. submontanum*. *M. aequale* has commonly been mistaken for some larger *Paleodictyon*. The distinction among them is not sharp and can be based on the prevalence of regular, hexagonal meshes in the latter. In *M. aequale*, most of the meshes are irregularly sub-pentagonal, sub-hexagonal or sub-heptagonal. In specimens with a small number of meshes, the distinction can be difficult. Therefore, some reservation in their determination is recommended.

The distinction between *Megagrapton irregulare* and *M. submontanum* is based on the curvature of the bordering ridges, which is larger in the latter. Moreover, the prevailing branching is different. It is mostly T-shaped in *M. irregulare,* Y-shaped in *M. aequale,* and characteristically curved in *M. submontanum* (Fig. 16). Nevertheless, these types of branches may occur subordinately in any of the ichnospecies, including the holotypes of *M. irregulare* an *M. submontanum*. Trends in morphometric parameters of *M. irregulare* and *M. submontanum* are almost the same (Fig. 12A). These two ichnospecies should be treated rather as endmembers, not sharply bounded entities, whose fields of parameters partly overlap (Fig. 12B).

The differences in morphometric parameters of *Megagrapton aequale* between regions or formations (Table 1) and even within the same lithostratigraphic units, e.g., between two different sections as between the Ardagani-3 and Ormotsi-1 sections (Fig. 9A), are hard to interpret. Differences in ontogenetic development, ecological conditions, and the taxonomy of tracemakers producing the same trace may be invoked, but none of the factors can be pointed to as the only convincing one. Even larger differences in morphometric parameters are present in *M. irregulare* and *M. submontanum.* The mesh size may differ by an order of magnitude in these ichnospecies. However, the largest specimens, with meshes wider than 80 mm, are rare. Differences in the parameters within single specimens or between specimens from the same bedding plane can be large but coefficients of correlation (r) and determinations (r^2) between maximum width of meshes (*mv*) and width of bordering ridges (*br*) are very low. The coefficients are higher for specimens from a larger number of beds from regions and/or formations (Table 1 and Fig. 9). The coefficients r for total number of measured specimens of *M. aequale*, *M. irregulare* and *M. submontanum* are 0.51, 0.54, and 0.69, respectively; the coefficients r^2 are 0.44, 0.29, and 0.47, respectively. This shows the bordering ridges tend to be thicker in specimens with larger meshes, but this tendency is not strong. This suggests that ontogenetic development plays some role but is not the dominant factor in mesh morphology. Width of the bordering ridges should treated with some caution because it depends on preservation processes, particularly the intersection of the original tunnel with the bedding plane caused by erosion on the deep-sea floor. That is, the intersection does not necessarily run through the widest section of the tunnel. Moreover, the tunnel can be widened by erosion (Monaco, 2008) or pinched by sediment creep. Extreme values that depart from the trend can be suspected as due to such factors. It seems that the most reliable width of the bordering ridges – which corresponds to the diameter of the original tunnel – is closer to the maximum values than to the minimum.

Megagrapton belongs to the graphoglyptids, which are relatively small, regular, largely horizontal “patterned” traces (Fuchs, 1895; Seilacher, 1977). Preservation of *Megagrapton,* notably its smooth tunnels without nodes suggesting vertical or oblique shafts, can be considered as evidence of a rather small number of openings (i.e., shafts) connecting the horizontal burrow system with the sediment surface. This fits with the idea that the burrow system is not a farming trace but rather a trap for small organisms, similar to *Cosmorhaphe* (Seilacher, 1977). Such burrows are distinguished as irretichnia, which are treated as a subcategory of praedichnia (Lehane and Ekdale, 2013), in contrast to other graphoglyptids related to farming of microbes as suggested by several openings (category agrichnia, Ekdale, 1985).

An interesting case is exemplified by the specimen illustrated in Figure 8E, where *Megagrapton aequale* is connected with *Paleodictyon* at the same level as the lower bedding surface. This could be accidental and caused by erosion exhuming two different but neighbouring burrow systems. The burrow systems were cast on the same sandstone sole. However, it is not excluded that the tracemaker of one burrow system captured the burrow system of the other. Both are networks, one regular (*Paleodictyon*) and the other irregular (*Megagrapton*), and their function could be the same after the capturing.

Megagrapton is a characteristic trace fossil of the Nereites ichnofacies, especially the *Paleodictyon* ichnosubfacies (Uchman and Wetzel, 2012). This is the case for *M. aequale* in the sections studied in the the Lesser Caucasus, where it co-occurs with several graphoglyptids (*Belorhaphe, Helminthorhaphe, Urohelminthoida, Protopaleodictyon, Paleodictyon;* see the comments on *M. aequale* in the systematic parts; Figs. 3 and 4). *M. aequale* occurs in the upper part of the Aradagani-3 section, which is characterized by abundance of heterolithic deposit intercalations and by the increased diversity of trace fossils (Fig. 4). The heterolithic deposits may be overbank deposits. The presence of debrites and slumps suggests proximity to the lower slope (e.g., Pickering and Corregidor, 2005). Probably the Ardagani-3 section represents a channelized depositional system at the toe of the slope. *M. aequale* from other formations occurs in deep-sea fan depositional systems, including in the type area, i.e. the Upper Cretaceous-Eocene flysch deposits of the Zumaya section (e.g., Crimes, 1977; Leszczyński, 1991; Cummings and Hodgson, 2011). The same holds for deep-sea turbiditic deposits in the Julian Prealps (Tunis and Uchman, 1996a; Marincić et al., 1996), Istria (Tunis and Uchman, 1996b), the Hecho Group in the southern Pyrenees (Uchman, 2021), the Kulm deposits in Moravia (Mikuláš et al., 2004) and other areas or formations. Other ichnospecies of *Megagrapton* occur in turbidites in distal lobes (e.g., Adserá et al., 2020), overchannel (Buatois et al., 2001), interlobe, fan fringe (e.g., Cummings and Hodgson, 2011) and basin floor (e.g., Uchman, 2001) or slope apron facies (Demircan and Uchman, 2016).

CONCLUSIONS

Among the eleven named ichnospecies of *Megagrapton* Książkiewicz, 1968, only *M. irregulare* Książkiewicz, 1968, *M. submontanum* (Azpeitia Moros, 1933), and *M. aequale* Seilacher, 1977 are recommended for further use; their diagnoses are emended or modified herein. They are differentiated on the basis of the prevailing shape of meshes. The recommended ichnospecies of *Megagrapton* show a wide range of morphometric parameters. A neotype is of designated for *M. aequale*. This ichnospecies ranges from lower Cambrian to upper Miocene deep-sea turbiditic deposits, mostly in the Paleogene. *Paleodictyon imperfectum* Seilacher, 1977 is included in *M. aequale* as the ichnosubspecies *M. a. imperfectum*. *Irredictyon chaos* Vialov, 1972 is included in *M. irregulare* as the ichnosubspecies *M. i. chaos*. *Megagrapton* represents a subsurface burrow network, which probably was a trap for small organisms (ethological subcategory irretichnia). *Megagrapton* is a typical representative of the Nereites ichnofacies, especially the Paleodictyon ichnosubfacies. It occurs in various parts of the deep-sea depositional system, mostly in packages of thin and medium beds of fine-grained turbiditic sandstones.

Acknowledgements. This works was supported by the Shota Rustaveli National Science Foundation of Georgia (SRNSFG) [Grant number FR-18-3765 – Ichnology and Sedimentology of the Paleocene-Lower Eocene Sediments in the Achara-Trialeti Fold-Thrust Belt, Georgia]. The photograph of the holotype of *Megagrapton aequale* was made by A. Fatz and provided by A. Krahl and J. Nebelsick (all from the Department of Earth Sciences, Tübingen University). The photograph of the holotype of *Paleodictyon imperfectum* and information about it was provided by F. Bowyer from the University of Edinburgh. The photograph of the specimen in Figure 8 was provided by T. Słomka (AGH University of Science and Technology, Kraków, Poland). Data provided from several collections by A. Uchman were obtained during researches supported by the Alexander von Humboldt Foundation (Germany), Jagiellonian University (Poland), and the Fondazione Luigi, Cesare e Liliana Bertora (Italy). We thank A.K. Rindsberg (University of West Alabama) and D. Knaust (Stavanger) for helpful reviews, which improved the paper.

REFERENCES

Adamia, S. ed., 2004. Geological Map of Georgia (scale 1:500.000). Georgian Department of Geology, Union Geo-Eco, Tbilisi, Georgia.

Adamia, S., Zakariadze, G., Lordkipanidze, M., Salukvadze, G., 1974. The geological structure of Achara (in Russian). In: Problems of the Geology of the Achara-Trialeti (eds. P. Gamkrelidze and M. Rubinshtein). Proceedings of the Institute of Geology of the Academy of Sciences of the GSSR, “Metsniereba”, Tbilisi, **44**: 60–69.

Adamia, S., Alania, V., Ananiashvili, G., Bombolakis, E., Chichua, G., Girshiashvili, D., Martin, R., Tatarashvili, L., 2002. Late Mesozoic-Cenozoic geodynamic evolution of the eastern Georgian oil-gas bearing basins. Geologica Carpathica, **53**: 155–159.

Adamia, S., Alania, V., Chabukiani, A., Chagelishvili, R., Enukidze, O, Jaoshvili, G., Razmadze, A., Sadradze, N., 2011. Tectonic setting of Georgia (Caucasus). In: Abstracts of 3rd International Symposium on the Geology of the Black Sea Region. Bucharest, Romania (eds. G. Oaie, A. Seghedi, V. Yanko-Hombach, B. Popescu, M. Micu and N. Panin). Supplement to Geo-Eko-Marina, **17**: 11–13.

Adamia, S., Chkhotua, T., Gavtadze, T., Lebanidze, Z., Lursmanashvili, N., Sadradze, N., Zakaraia, D., Zakariadze, G., 2015. Tectonic setting of Georgia–Eastern Black Sea: a review. Geological Society Special Publications, **428**: 10–40.

Adserá, P., Belaústegui, Z., Uchman, A., 2020. *Estrellichnus jacaensis* from the Eocene Jaca Basin (NE Spain): new locality and new ethological interpretation. Lethaia, **53**: 129–143.

Alania, V., Chabukiani, A., Chagelishvili, R., Enukidze, O., Gogrichiani, K., Razmadze, A., Tsereteli, N., 2017. Growth structures, piggyback basins and growth strata of Georgian part of Kura foreland fold and thrust belt: implication for Late Alpine kinematic evolution. Geological Society Special Publications, **428**: 171–185.

Alania, V., Kvavadze, N., Enukidze, O., Beridze, T., Gventsadze, A., Tevzadze, N., 2021. Seismic interpretation of southern part of the eastern Achara-Trialeti Fold-and-Thrust Belt, Georgia. Bulletin of the Georgian National Academy of Sciences, **15**: 57–62.

Azpeitia Moros, F., 1933. Datos para el estudio paleontlógico del Flysch de la Costa Cantábrica y de algunos otros puntos de España. Boletín del Instituto Geologico y Minero de España, **53**: 1–65.

Banks, C., Robinson, A.G., Williams, M., 1997. Structure and regional tectonics of the Achara-Trialeti fold belt and the adjacent Rioni and Kartli foreland basins, Republic of Georgia. AAPG Memoir, **68**: 331–346.

Beradze, R., Gamrekeli, G., Bandzava, D., Kavtaradze, S., Areshidze, R., Labadze, I., Zhgenti, A., Geguchadze, L., Lebanidze, Z., Sabanadze, M., Sagiridze, L., 1985. Report (#16838) of the Trialeti geological-prospecting party about 1:25 000 scale mapping within the sheets K-38-75-Б-в,г and K-38-75-Г-а,δ (the central part of the Achara-Trialeti economic region) on the basis of conducted works in 1982–1985, Geological-Geophysical expedition for regional exploration, Trialetian geological mapping party, Geological Department of the Ministry of Geology of the Georgian SSR, Tbilisi, 1-400 (in Russian). Catalogue of the geological fund [archive] of the National Agency of Mineral Resources, Georgia, https://namgeofund.archivalservices.gov.ge/geofond/item_detailed/6967

Beridze, T., 2019. Middle Eocene submarine mass-transport deposits of Tbilisi environs (eastern Achara-Trialeti fold and thrust belt, Georgia). In: Sedimentology to face societal challenges on risk, resources and record of the past. 34th International Meeting of Sedimentology, Rome 10–12 September, 2019, Abstract Book. Sapienza Università di Roma. Session 7 F-476.

Beridze, T., Lebanidze, Z., Uchman, A., Lobzhanidze, K., Khutsishvili, S., Chagelishvili, R., Kobakhidze, N., Makadze, D., Khundadze, N., Koiava, K., 2021. Ichnological-sedimentological indicators of deep-sea environment in Lower Eocene deposits of the Borjomi region (Georgia). In: 35th Meeting of Sedimentology: Prague, Czech Republic, 21–25 June 2021, Book of Abstracts (eds. O. Bábek and S. Vodrážková): 55. Palacký University of Olomouc, Olomouc.

Buatois, L.A., Mángano, M.G., Sylvester, Z., 2001. A diverse deep-marine ichnofauna from the Eocene Tarcau Sandstone of the eastern Carpathians, Romania. Ichnos, **8**: 23–62.

Crimes, T.P., 1977. Trace fossils of an Eocene deep-sea fan, northern Spain. Geological Journal Special Issue, **9**: 71–90.

Crimes, T.P., McCall, G.J.H., 1995. A diverse ichnofauna from Eocene-Miocene rocks of the Makran Range (S.E. Iran). Ichnos, **3**: 231–258.

Cummings, J.P., Hodgson, D.M., 2011. Assessing controls on the distribution of ichnotaxa in submarine fan environments, the Basque Basin, Northern Spain. Sedimentary Geology, **239**: 162–187.

D'Alessandro, A., 1981. Processi tafonomici e distribuzione delle trace fossili nel flysch di Gorgolione (Appennino Meridionale). Rivista Italiana di Paleontologia e Stratigrafia, **87**: 511–560.

Demircan, H., Uchman, A., 2016. Ichnology of prodelta deposits of the Mezardere Formation (late Eocene–early Oligocene) in the Gökçeada island, western Turkey. Geodinamica Acta, **28**: 86–100.

Demircan, H., Görmüş, M., 2020. Ichnology of Upper Cretaceous–lower Palaeogene deep-sea deposits in the Haymana Basin of Central Anatolia. Annales Societatis Geologorum, **90**: 463–493.

Ekdale, A.A., 1985. Paleoecology of the marine endobenthos. Palaeogeography, Palaeoclimatology, Palaeoecology, **50**: 63–81.

Ekdale, A., Gibert, J.M., 2014. Late Miocene deep-sea trace fossil associations in the Vera Basin, Almería, Southeastern Spain. Spanish Journal of Palaeontology, **29**: 95–104.

Fuchs, T., 1895. Studien über Fucoiden und Hieroglyphen. Denkschriften der k.k. Akademie der Wissenschaften in Wien, mathematisch-naturwissenschaftliche Classe, **62**: 369–448.

Gamkrelidze, P., 1949. Geological structure of the Adjara-Trialetian folded system (in Russian). Academy of Sciences of Georgia Press, Tbilisi.

Gamkrelidze, P. ed., 1964. Geology of the USSR. Georgian SSR (in Russian). Nedra, Moscow.

Geinitz, H.B., 1867. Die organischen Überreste im Dachschiefer von Wurzbach bei Lobenstein. Nova Acta Academiae Caesarea Leopoldino-Carolinae, Germanicae Naturae Curiosorum, **33**: 1–24.

Ghare, M.A., Badve, R.M., 1977. Trace fossils from the Vindhayans of Chambal Valley. Biovigyanam, **3**: 205–215.

Göppert, H.R., 1842. Über die fossile Flora der Quadersandstein formation in Schlesien, als erster Beitrag zur Flora der Tertiärgebilde. Nova Acta Academiae Caesarea Leopoldino-Carolinae, Germanicae Naturae Curiosorum, **19**: 97–134,

Häntzschel, W., 1975. Trace fossils and problematica. In: Treatise on Invertebrate Paleontology, part W, Miscellanea, Supplement I (ed. C. Teichert): W1-W269. Geological Society of America, Boulder (Colorado), and University of Kansas, Lawrence (Kansas).

Heard, T.G., Pickering, K.T., 2008. Trace fossils as diagnostic indicators of deep-marine environments, middle Eocene Ainsa--Jaca basin, Spanish Pyrenees. Sedimentology, **55**: 809–844.

Kappel, J., 2003. Ichnofossilien im Campanium des SE-Münsterlands. Münsterische Forschungen zur Geologie und Paläontologie, **96**: 1–163.

Khaidam, K.S., Rajkumar, H.S., Soibam, I., 2015. Attribute of trace fossils of Laisong flysch sediments, Manipur, India. Journal of Earth System Science, **124**: 1085–1113.

Kim, Y.-Y., Seo, Y.-S., Park, S.-I., 1992. Trace fossils from the Yeongheung Formation, Yeongweol, Korea. The Journal of the Korean Earth Science Society, **13**: 313–326.

Kozur, H.W., Krainer, K., Mostler, H., 1996. Ichnology and sedimentology of the Early Permian deep-water deposits from the Lercara-Roccapalumba area (western Sicily, Italy). Facies, **34**: 123–150.

Kilibarda, Z., Schassburger, A., 2018. A diverse deep-sea trace fossil assemblage from the Adriatic Flysch Formation (middle Eocene–middle Miocene), Montenegro (central Mediterranean. Palaeogeography, Palaeoclimatology, Palaeoecology, **506**: 112–127.

Krawczyk, A.J., Słomka, T., 1981. Trace-fossil *Paleodictyon* from the Szlachtowa Formation (?Upper Toarcian–Lower Aalenian of the Pieniny Klippen Belt, Poland) (in Polish with English summary). Studia Geologica Polonica, **70**: 67–71.

Książkiewicz, M., 1958. Stratigraphy of the Magura Series in the Średni Beskid (Carpathians) (in Polish with English summary). Biuletyn Instytutu Geologicznego, **153**: 43–96.

Książkiewicz, M., 1968. On some problematic organic traces from the Flysch of the Polish Carpathians. Part 3 (in Polish with English summary). Rocznik Polskiego Towarzystwa Geologicznego, **38**: 3–17.

Książkiewicz, M., 1977. Trace fossils in the Flysch of the Polish Carpathians. Palaeontologia Polonica, **36**: 1–208.

Lebanidze, Z., Beridze, T., Kobakhidze, N., Khutsishvili, S., Chagelishvili, R., Koiava, K., Khundadze, N., Uchman, A., 2019. Trace fossils in Paleocene-Lower Eocene deep-sea sediments ("Borjomi Flysch") of the Achara-Trialeti Fold-Thrust Belt. In: Sedimentology to face societal challenges on risk, resources and record of the pas, 34th International Meeting of Sedimentology, Rome 10–12 September, 2019, Abstract Book. Sapienza Università di Roma. Session 8.A-346.

Lehane, J.R., Ekdale, A.A., 2013. Pitfalls, traps, and webs in ichnology: traces and trace fossils of an understudied behavioral strategy. Palaeogeography, Palaeoclimatology, Palaeoecology, **375**: 59–69.

Leszczyński, S., 1991. Ichnocoenosis versus sediment colour in Upper Albian to lower Eocene turbidites, Guipúzcoan province, northern Spain. Palaeogeography, Palaeoclimatology, Palaeoecology, **100**: 251–265.

López Cabrera, M.I., Olivero, E.B., 2014. *Ophiomorpha irregulaire* and associated trace fossils from the Upper Cretaceous of Patagonia, Argentina: palaeogeographical and ethological significance. Spanish Journal of Palaeontology, **29**: 33–44.

López Cabrera, M.I., Olivero, E.B., Carmona, N.B., Ponce, J.J., 2008. Cenozoic trace fossils of the Cruziana, Zoophycos and Nereites ichnofacies from the Fuegian Andes, Argentina. Ameghiniana, **45**: 377–392.

Lordkipanidze, M., Meliksetian, B., Djarbashian, R., 1989. Mesozoic-Cenozoic magmatic evolution of the Pontian Crimean-Caucasian region. Mémoires de la Société géologique de France, Nouvelle Série, **154**: 103–124.

Luo, M., Shi, G.R., Hu, S., Benton, M.J., Chen, Z.-Q., Huang, J., Zhang, Q., Zhou, C., Wen, W., 2019. Early Middle Triassic trace fossils from the Luoping Biota, southwestern China: evidence of recovery from mass extinction. Palaeogeography, Palaeoclimatology, Palaeoecology, **515**: 6–22.

Macsotay, O., 1967. Huellas problemáticas y su valor paleoecológico en Venezuela. GEOS Revista Venezoelana de Ciencias de la Terra, **16**: 7–39.

Madon, M., 2021. Deep-sea trace fossils in the West Crocker Formation, Sabah (Malaysia), and their palaeoenvironmental significance. Bulletin of the Geological Society of Malaysia, **71**: 23–46.

Marinčić, S., Šparica, M., Tunis, G., Uchman, A., 1996. The Eocene flysch deposits of the Istrian Peninsula in Croatia and Slovenia: regional, stratigraphic, sedimentological and ichnological analyses. Annales for Istrian and Mediterranean Studies, **9**: 139–156.

Miller, W., III, 1988. Giant *Bathysiphon* (Foraminiferida) from Cretaceous turbidites, Northern California. Lethaia, **21**: 363–374.

Mikuláš, R., Lehotský, T., Bábek, O., 2004. Trace fossils of the Moravice Formation from the southern Nízký Jeseník Mts. (Lower Carboniferous, Culm facies; Moravia, Czech Republic). Bulletin of Geosciences, **79**: 81–98.

Monaco, P., 2008. Taphonomic features of *Paleodictyon* and other graphoglyptid trace fossils in Oligo-Miocene thin-bedded turbidites, Northern Apennines, Italy. Palaios, **23**: 667–682.

Monaco, P., Milighetti, M., Checconi, A., 2010. Ichnocoenosis in the Oligocene to Miocene foredeep basins (Northern Apennines, central Italy) and their relation to turbidite deposition. Acta Geologica Polonica, **60**: 53–70.

Monaco, P., Trecci, T., 2014. Ichnocoenoses in the Macigno turbidite basin system, Lower Miocene, Trasimeno (Umbrian Apennines, Italy). Italian Journal of Geosciences, **133**: 116–130.

Nadareishvili, G., 1999. Cretaceous volcanic formations of Georgia (in Russian). Proceedings of the Geological Institution of the Academy of Sciences of GSRR, **114**: 79–194.

Nielsen, J.K., Görmüş, M., Uysal, K., Kanbur, S., 2010. First records of trace fossils from the Lake District, southwestern Turkey. Bulletin of Geosciences, **85**: 691–708.

Obruchev, S., 1923. Geological assay on Borjomi (in Russian). Trudy Instituta Prikladnoy Mineralogii i Petrografii, vypusk **1**: 104.

Orłowski, S., 1968. Cambrian of the Łysogóry Anticline in the Holy Cross Mountains (in Polish with English summary). Biuletyn Geologiczny, **10**: 195–221.

Pacześna, J., 1985. Ichnogenus *Paleodictyon* Meneghini from the Lower Cambrian of Zbilutka (Góry Świętokrzyskie Mts) (in Polish with English summary). Kwartalnik Geologiczny, **29** (3/4): 589–596.

Papava, D., 1966. Geological structure of the eastern area of the Trialethi Ridge (in relation to perspectives of oil-gas content) (in Russian). Thesis for the degree of candidate of geological and mineralogical sciences. Geological Institute of the Academy of Sciences of GSSR, Ministry of Oil Industry of the USSR, Trust “Gruzneft”, Tbilisi.

Pfeiffer, H., 1968. Die Spurenfossilien des Kulms (Dinants) und Devons der Frankenwälder Querzone (Thüringen). Jahrbuch der Geologie, **2**: 651–717.

Pickerill, R.K., Fyffe, L.R., Forbes, W.H., 1988. Late Ordovician Early Silurian trace fossils from the Matapedia Group, Tobique River, western New Brunswick, Canada. II. Additional discoveries with descriptions and comments. Maritime Sediments and Atlantic Geology, **24**: 139–148.

Pickering, J.T., Corregidor, I., 2005. Mass transport complexes and tectonic control on confined basin-floor submarine fans, Middle Eocene, south Spanish Pyrenees. Geological Society Special Publications, **244**: 51–74.

Rodríguez-Tovar, F.J., Uchman, A., Payros, A., Orue-Etxebarria, X., Apellaniz, E., Molina, E., 2010. Sea-level dynamics and palaeoecological factors affecting trace fossil distribution in Eocene turbiditic deposits (Gorrondatxe section, N Spain). Palaeogeography, Palaeoclimatology, Palaeoecology, **285**: 50–65.

Rodríguez-Tovar, F.J., Pińuela, L., García-Ramos, J.C., 2016. Trace fossils assemblages from the Cenozoic “Flysch Units” of the Campo de Gibraltar Complex (southern Spain). Ichnos, **23**: 53–70.

Sabhaya, M.B., Patel, R.A., Solanki, P.M., 2021. Palaeoichnology of Jurassic sequence of Jara Dome, Kachchh, western India. Science, Technology and Development, **10**: 41–50.

Sacco, F., 1888. Note di paleoicnologia italiana. Atti della Societá Italiana di Scienze Naturali, **31**: 151–192.

Sacco, F., 1939. *Paleodictyon*. Memorie della Reale Accademia delle Scienze di Torino, **69**: 267–286.

Savi, P., Meneghini, G.G., 1850. Osservazioni stratigrafiche e paleontologische concernati la geologia della Toscana e dei paesi limitrofi. – Appendix. In: Memoria sulla struttura geologica delle Alpi, degli Apennini e dei Carpazi (ed. R.I. Murchison): 246–528. Stamperia granducale, Firenze.

Sedgwick, A., 1848. On the organic remains found in the Skiddaw Slate, with some remarks on the classification of the older rocks of Cumberland and Westmoreland. The Quarterly Journal of the Geological Society of London, **4**: 216–335.

Seilacher, A., 1977. Pattern analysis of *Paleodictyon* and related trace fossils. Geological Journal, Special Issue, **9**: 289–334.

Simpson, F., 1969. Interfacial assemblages of foraminifera in the Carpathian Flysch. Rocznik Polskiego Towarzystwa Geologicznego, **39**: 471–486.

Stepanek, J., Geyer, G., 1989. Spurenfossilien aus dem Kulm (Unterkarbon) des Frankenwaldes. Beringeria, **1**: 1–55.

Schweigert, G., 1998. Die Spurenfauna des Nusplinger Plattenkalks (Oberjura, Schwäbische Alb). Stuttgarter Beiträge zur Naturkunde, Serie B (Geologie und Paläontologie), **262**: 1–47.

Sosson, M., Stephenson, S., Sheremet, Y., Rolland, Y., Adamia, S., Melkonian, R., Kangarli, T., Yegorova, T., Avagyan, A., Galoyan, G., Danelian, T., Hässig, M., Meijers, M., Müller, C., Sahakyan, L., Sadradze, N., Alania, V., Enukidze, O., Mosar, J., 2016. The Eastern Black Sea–Caucasus region during Cretaceous: new evidence to constrain its tectonic evolution. Comptes Rendus Geosciences, **348**: 23–32.

The International Code of Zoological Nomenclature, 1999. The International Trust for Zoological Nomenclature 1999; https://www.iczn.org/the-code/the-code-online/

Tunis, G., Uchman, A., 1996a. Trace fossil and facies changes in the Upper Cretaceous-Middle Eocene flysch deposits of the Julian Prealps (Italy and Slovenia): consequences of regional and world-wide changes. Ichnos, **4**: 169–190.

Tunis, G., Uchman, A., 1996b. Ichnology of the Eocene flysch deposits in the Istria peninsula, Croatia and Slovenia. Ichnos, **5**: 1–22.

Uchman, A., 1995. Taxonomy and palaeoecology of flysch trace fossils: the Marnoso-arenacea Formation and associated facies (Miocene, Northern Apennines, Italy). Beringeria, **15**: 3–115.

Uchman, A., 1998. Taxonomy and ethology of flysch trace fossils: a revision of the Marian Książkiewicz collection and studies of complementary material. Annales Societatis Geologorum Poloniae, **68**: 105–218.

Uchman, A., 2001. Eocene flysch trace fossils from the Hecho Group of the Pyrenees, northern Spain. Beringeria, **28**: 3–41.

Uchman, A., 2009. The *Ophiomorpha rudis* ichnosubfacies of the Nereites ichnofacies: characteristics and constraints. Palaeogeography, Palaeoclimatology, Palaeoecology, **276**: 107–119.

Uchman, A., Wetzel, A., 2012. Deep-sea fans. Developments in Sedimentology, **64**: 643–671.

Uchman, A., Hanken, N.-M., Binns, R., 2005. Ordovician bathyal trace fossils from metasiliciclastics in central Norway and their sedimentological and paleogeographical implications. Ichnos, **12**: 105–133.

Uchman, A., Lebanidze, Z., Beridze, T., Kobakhidze, N., Lobzhanidze, K., Khutsishvili, S., Chagelishvili, R., Makadze, D., Koiava, K., Khundadze, N., 2020. Abundant trace fossil *Polykampton* in Palaeogene deep-sea flysch deposits of the Lesser Caucasus in Georgia: palaeoecological and palaeoenvironmental implications. Palaeogeography, Palaeoclimatology, Palaeoecology, **558**: 109958.

Vass, D., 1971. Présence de *Paleodictyon* (Problematica) dans le Numidien de la Tunisie septentrionale. Notes Service Géologique de Tunisie, **34**: 47–52.

Vialov, O.S., 1972. Bioglify iz paleogena Dagestana (in Russian). Paleontologicheskiy Sbornik, **9**: 75–80.

Warchoł, M., Leszczyński, S., 2009. Trace fossils from Silurian and Devonian turbidites of the Chauvay area, southern Tien Shan, Kyrgyzstan. Annales Societatis Geologorum Poloniae, **79**: 1–11.

Wetzel, A., Blechschmidt, I., Uchman, A., Matter, A., 2007. A highly diverse ichnofauna in Late Triassic deep-sea fan deposits of Oman. Palaios, **22**: 567–576.

Wetzel, A., Uchman, A., 1997. Ichnology of deep-sea fan overbank deposits of the Ganei Slates (Eocene, Switzerland) – a classical flysch trace fossil locality studied first by Oswald Heer. Ichnos, **5**: 139–162.

Wilson, R.D., Schieber, J., Stewart, C.J., 2021. The discovery of widespread agrichnia traces in Devonian black shales of North America: another chapter in the evolving understanding of a "not so anoxic" ancient sea. PalZ (Paläontologische Zeitschrift), **95**: 661–681.

Yang, S., Song, Z., 1985. Middle-Upper Triassic trace fossils from Zhada, Ngari, southwest Xizang (Tibet), and its geologic significance. Geology of Xizang (Tibet Geology), **1**: 1–14.

Yang, S., Zhang, J., Yang, M., 2004. Trace Fossils of China. Beijing.

Yilmaz, A., Adamia, S., Lordkipanidze, M., Yilmaz, T., Kurt, I., Abesadze, G., Lazarashvili, T., Beradze, R., Nadirashvili, R., Kuloshvili, S., Salukvadze, N., Özkan, M., 2001. A study of tectonic units of the area along Turkish-Georgian border. In: Geological Studies of the Area Along Turkish-Georgian Border (eds. A. Yilmaz, T. Engin, S. Adamia and T. Lazarashvili). State Department of Geology – Georgia, Geological Institute of the Academia of Sciences-Georgia, Ankara.

Zakariadze, G., Dilek, Y., Adamia, S., Oberhänsli, R., Karpenko, S., Bazylev, B., Solov'eva, N., 2007. Geochemistry and geochronology of the Neoproterozoic Pan-African Transcaucasian Massif (Republic of Georgia) and implications for island-arc evolution of the late Precambrian Arabian–Nubian Shield. Gondwana Research, **11**: 92–108.

Zakariadze, G., Karamata, S., Korikovsky, S., Ariskin, A., Adamia, S., Chkhotua, T., Sergeev, S., Solov'eva, N., 2012. The Early-Middle Paleozoic oceanic events along the southern European margin: the Deli Jovan Ophiolite Massif (NE Serbia) and paleooceanic zones of the Great Caucasus. Turkish Journal of Earth Sciences, **21**: 635–668.

Zayats, P.P., Nazarenko, O.V., Ruban, D.A., 2015. New findings of ichnofossils in the Bagovskaya Formation (Lower Jurassic) of the Western Caucasus. Izvestya Vysshikh Uchebnikh Zaviedenyi, Geologia i Razvedka, **5**: 82–85.

Zhang, X., Shi, G.R., Gong, Y., 2008. Middle Jurassic trace fossils from the Ridang Formation in Sajia County, South Tibet, and their palaeoenvironmental significance. Facies, **54**: 45–60.